THE UNIVERSITY OF MANITOBA

MEASUREMENT AND MODELLING OF RADIO NOISE FROM ELECTRIC POWER LINES IN THE RURAL REGION SURROUNDING THE CITY OF WINNIPEG.

BY

MOHAMED TAREK GAD

A THESIS
SUBMITTED TO THE FACULTY OF GRADUATE STUDIES
IN PARTIAL FULFILLMENT OF THE REQUIREMENTS FOR THE DEGREE
OF MASTER OF SCIENCE

DEPARTMENT OF ELECTRICAL ENGINEERING

MAY 1980

WINNIPEG, MANITOBA

MEASUREMENT AND MODELLING OF RADIO NOISE FROM ELECTRIC POWER LINES IN THE RURAL REGION SURROUNDING THE CITY OF WINNIPEG

BY

MOHAMED TAREK GAD

A thesis submitted to the Faculty of Graduate Studies of the University of Manitoba in partial fulfillment of the requirements of the degree of

MASTER OF SCIENCE

© 1980

Permission has been granted to the LIBRARY OF THE UNIVERSITY OF MANITOBA to lend or sell copies of this thesis, to the NATIONAL LIBRARY OF CANADA to microfilm this thesis and to lend or sell copies of the film, and UNIVERSITY MICROFILMS to publish an abstract of this thesis.

The author reserves other publication rights, and neither the thesis nor extensive extracts from it may be printed or otherwise reproduced without the author's written permission.

ABSTRACT

The noise characteristics of transmission lines in the high frequency bands extending to 32 MHz are experimentally investigated. The noise emitted from transmission lines affecting radio reception is analysed with the use of a linear regression technique to model the various classes of power lines classified according to line voltage.

These models provide a tool to predict the performance of radio reception in the presence of power line interference. It was observed that noise levels were affected by the line voltage and the load conditions on the line.

ACKNOWLEDGEMENTS

The author wishes to express his appreciation to Professor E. Bridges for his continuous interest, helpful advice, cheerful and able guidance in all phases of this work. The author wishes also to express his appreciation to Dr. L. Shafai and Dr. W. R. Goddard for their valuable comments.

The financial assistance provided by the Communication Research Centre and the Department of Electrical Engineering of the University of Manitoba are gratefully acknowledged.

TABLE OF CONTENTS

LIST OF FIGURES

Figure page

LIST OF TABLES

Chapter I

INTRODUCTION

In the last two decades, the increasing need for transmission of large amounts of electrical energy over the long distances which separate generating stations from consumption centers, has resulted in the development and installation of transmission lines operating at very high voltages. At the same time, concern is also increasing regarding the environmental effects of such lines. One of these environmental factors is the radio interference (RI) generated by electromagnetic sources originating from the transmission lines. Generally, there are two sources of electromagnetic interference (EMI) associated with power lines. One of these is due to high voltage corona, the other is the result of gap discharge or microsparks [1].

The amount of electromagnetic interference generated by a power line is controlled to a large degree by the conductor radius and phase spacing. Choice of conductor radius and of phase spacing has a direct bearing upon the corona performance of the line [2]. The susceptibility of a line to the occurrence of gap discharges may also be related to conductor radius and phase spacing as well as to insulator type.

There are other factors which affect the electromagnetic performance of the line which cannot be eliminated by design. Weather conditions and the topology of the locale in which the line is erected constitute the two most important aspects over which the designer has little control.

The phenomenon of corona discharge is normally caused by small protrusions on the line conductors and by conductor surface contaminants such as water droplets, dirt and other material. The electric field at the protrusions is enhanced and produces corona at normal operating line voltages [3,4]. Corona is a faint glow that may be observed in the electrically overstressed air surrounding a power line component. The electric field intensity changes from space point to space point and is especially high adjacent to sharply curved surfaces such as those of protrusions. Upon raising the voltage of such surfaces, a critical level of the electric field may be exceeded and the physical processes causing corona will be initiated. When this happens, it is said that the corona onset level has been reached. A further increase in the applied voltage will result in an enhancement of the corona activity.

Design values of voltage gradients refer to smooth (non-stranded) conductors with clean surfaces and these values assume normal dielectric strength of air. In reality, conductors are stranded and they, along with other hardware, can become contaminated. Stranding and contamination constitute surface irregularities which cause local concentration of the electric field. As soon as this concentration exceeds the critical value of the voltage gradient (corona onset value), corona discharges will occur.

In addition to these processes, corona is also influenced (even more strongly) by weather effects. Corona onset voltage (for any given geometry) is determined by air density and humidity [5-7] . Corona voltage varies inversely with air density. Thus, it varies directly with air pressure and inversely with temperature [7]. When rain drops, ice or snow accumulate on conductors and on hardware surfaces, they also cause irregularities which increase the surface voltage gradient.

Corona discharge is accompanied by a variety of manifestations, such as chemical effects, primarily those of ionization of air components. Accoustical waves are also formed, as a consequence of molecular collisions and from avalanche formations during the discharge process. Also, there is electromagnetic radiation that accompanies the pulsative forms of discharges. Generally, all of the above constitute an energy loss, however, corona loss is not the only phenomenon that accompanies the occurrence of corona. Interference with communication facilities is the consequence of the electromagnetic radiation. This radiation, as well as corona loss, must be limited to an acceptable value as, otherwise, such a vital service as radio reception could be jeopardized.

The gap type sources of electromagnetic radiation can occur in insulators, at tie wires, between hardware parts, at small gaps between neutral or ground wires and hardware, and in electrical equipment that is defective, damaged or improperly designed or installed. Gap-type sources can and do occur frequently on overhead power lines; however, these can be found and eliminated when necessary. The gap type sources are produced by two electrically isolated surfaces charged by the action of an alternating electric field. When the potential difference between them increases until the dielectric withstand-strength of air is exceeded, the air in the gap breaks down. During the break down phase, charge is carried from one surface to the other, until their potentials are equalized and the arc is extinguished. The insulating strength of air is then re-established and the stage is set for the new charging process and for repetition of the breakdown [6]. The influence of weather conditions upon gap sources is found to be opposite of that upon corona activity. Water droplets of rain short out the minute gaps and thus prevent the discharge process.

EMI has a greater affect on the quality of radio reception in certain frequency ranges than in others. Reception in the AM broadcast frequency range is more susceptable to the presence of corona generated RI, than reception in other broadcast ranges. Electric power lines provide a natural path for EMI from the source to the receiver. This propagation mechanism is particularly important for the frequency range below about 30MHz, as the wave length is long in comparison with phase spacing[1].

Radio waves propagate through space in a number of modes termed as ground waves, sky waves and space or tropospheric waves. For broadcast and at lower frequencies, the propagation of radio signals is mainly accomplished by ground waves which are insensitive to weather conditions. However, these waves may be disturbed by natural electric discharges such as lightning which may increase the noise level significantly.

The quality of radio reception is a function of the signal to noise ratio, S/N, available to the receiver [8,9]. S/N is defined as the ratio of the average signal power to the average noise power in a given bandwidth. By reducing the noise level at the receiver input, the quality of reception improves.

The EMI emitted from power lines has been studied by others in order to determine the level of noise and its effect on radio, TV and communication services.

Lauber and Bertrand [10] measured the RI due to corona discharge from transmission lines over a seventeen day period in November 1976 at four sites in downtown Ottawa. They used a Singer electromagnetic interference meter, model NM37/57, along with a discone antenna and made measurements over a frequency range of 100-1000 MHz. This project was an extension of previous studies [11,12,13] on high frequency radio noise interference.

They obtained the antenna effective noise factor, F_a, and the voltage deviation, V_d (which will be defined in chapter two) for a discone antenna. In the frequency range used, an antenna of this type has greater gain than the vertical monopole antenna used in radio environment studies.

In his study Lauber [13] made an amplitude probability distribution (APD) measurement of the noise spectrum in the high frequency bands emitted from the 775 KV project at Apple Grove. He used a monopole antenna with a Singer noise interference meter, model NM26T, to carry out the measurements. He has shown that values for the noise parameters usually measured by radio interference meters, except for the quasi-peak parameter, could be obtained from the APD data. He concluded that the APD of the noise can be deduced from the measured root-mean-square noise voltage and its voltage deviation. He also showed that the inverse of this is true, that is to say, by measuring these two parameters one can predict the APD of the noise which is a measure of the performance of radio reception in the presence of transmission line EMI.

Herak and Kirk [14], in a project of the Department of Communication, studied transmission line noise in the city of Winnipeg during the summer of 1977. They were concerned with power line noise in the urban area and took measurements of the root-mean-square voltage (V_{rms}), the quasi-peak voltage (QP) and the field intensity voltage (FI) of the noise spectrum. They used a modified Singer NM25T (equivalent to an NM26T) meter for the frequency range of 185 KHz-30MHz and a Singer NM37/57 meter for higher frequency bands up to 950 MHz. They measured F_a fifty feet away from the outer conductor of the power line and applied linear regression to several samples of F_a in order to obtain the noise prediction at that distance. For the lines they surveyed, they concluded that, at about 1 MHz, the S/N ratio of radio reception ranges from 25 to 29 dB, adequate for class B reception. Their measurement procedure will be discussed in another part of this thesis.

This study, as a part of the central Canada region study on Radio Interference from electric power lines by E.Bridges, W.R.Goddard, T.Gad and W.M.Boerner. [15], [16], investigates the properties of electromagnetic noise associated with power lines in the rural region surrounding the City of Winnipeg. Measurements of this noise were performed in order to determine the dependance of EMI on such parameters as frequency, lateral profile, line voltage and weather conditions. Fourteen test sites were selected on the Manitoba Hydro system. These sites were chosen such that interference from other sources (neighbouring power lines, commercial radio stations) was minimal. Accessability during poor weather conditions was also a factor influencing site selection. The AC transmission lines ranged in line voltage from 12 to 230 KV. One HVDC site on a 450 KV line was also chosen. An average of ten visits were made at each site over a one year period. Weather information and line operating conditions at each visit were obtained by mobile telephone.

Measurements of rms noise voltage across 50 ohms, V_{rms} and the voltage deviation, V_d, were made using a Singer NM26T meter (which has a noise bandwidth of 3.36 KHz), coupled through a matching network, to a Singer 9 foot long monopole rod antenna. Nine test frequencies in the range from 0.3 to 32 MHz were selected. Reading were taken at each of the selected frequencies at a location 50 feet perpendicular from the power line. At certain sites that produced significant noise levels a lateral profile was obtained by moving the measurement station (a van) to several locations extending out to 500 feet from the center of the line. The data obtained were entered into computer files.

Since power line noise is a random phenomenon, only a statistical analysis of its characteristics will yield meaningful results [19]. In this study, computer programs were developed to perform this analysis on the collected data base of the voltage deviation, V_d , and for the effective antenna noise factor, F_a , calculation. The linear regression technique [17]-[19] is applied to construct prediction models for the various classes of power lines, classified according to line voltage. The models are obtained from data collected during the two major seasons, thus they describe noise emission in different weather conditions.

These models can be used to predict the noise levels from any one of the different classes of transmission lines erected in the same environment as that surveyed. According to these models, the performance of radio systems operating in a power line environment can also be predicted.

The second chapter presents the theoretical background necessary for obtaining the various noise parameters used. The noise parameter definitions are according to the international radio consultative committee, C.C.I.R., Doc. 322 [20]. In chapter three, the measurement plan, the instrumentation and the measurement procedure, along with the site selection process, are presented. Chapter four describes the methods used to process the collected data base for F_a and V_d, the computer programs prepared to analyse the data and the results of this study. The applications of the models to radio reception are also presented in chapter four. Chapter five introduces the summary and conclusions of this study.

Chapter II

DEFINITIONS AND THEORY OF ELECTROMAGNETIC INTERFERENCE PREDICTION PARAMETERS

2.1 INTRODUCTION

In this chapter, the parameters most generally used to predict power line noise emission are defined and explained. The definitions of other measurement factors applicable to this study are also presented.

Generally, it is agreed that no single noise parameter can satisfactorly characterize Radio Interference [20]. However, one parameter which is universally used to compare noise produced from different sources and which is easily related to most of the other parameters used, is the effective antenna noise factor F_a [20]. The definition and relationship of F_a to the measured root mean square noise voltage, V_{rms}, is given in this chapter. Also defined is the voltage deviation V_d, another important parameter used, along with V_{rms}, to obtain the amplitude probability distribution (APD) of the noise spectrum.

The electromagnetic emission from power lines is a random phenomenon thus, only a statistical analysis of this phenomenon produces meaningful results [13]. The regression model is a useful technique to estimate the values of this noise emission. Using the regression model, one can predict the levels of the noise emitted from a particular power line and the performance of radio reception in the presence of the particular power line.

2.2 THE EFFECTIVE ANTENNA NOISE FACTOR

The antenna noise factor, f_a, is defined as the ratio of the noise power available from a lossless equivalent antenna to a reference thermal noise power.

Thus:

$$f_a = \frac{P}{kTB} \tag{1}$$

where

P is the mean noise power available from an equivalent lossless antenna (watts),

k is Boltzman's constant (1.38×10^{-23} Joules/K),

T is the reference temperature (Kelvin), $288^{\circ}K$,

B is the effective receiver noise bandwidth (Hz).

From equation (1), it is seen that f_a is a dimensionless factor, alternatively, one may define the quantity

$$F_a \text{ (dB)} = 10 \log f_a$$

which is the noise power per unit bandwidth in dB relative to kT. Equation (1) can be written as:

$$F_a(dB) = P(dBW) - B(dBHz) + 204 \quad . \tag{3}$$

The power density received by a lossless antenna is given by:

$$p = \frac{E^2}{\eta} \tag{4}$$

where

E is the electric field strength (V/m),

η is the free space impedance (ohms).

The electric field strength is given in terms of the effective antenna height H, by:

$$E = \frac{V}{2H} \tag{5}$$

where V is the voltage induced at the antenna terminals. Substituting from (5) into (4) gives the power density :

$$p = \frac{V^2}{4H^2} \frac{1}{\eta} \quad . \tag{6}$$

The power received by the antenna P is equal to the power density of the lossless antenna multiplied by the effective antenna aperture A which is given by:

$$A = \frac{\lambda^2 D}{4\pi} \quad . \tag{7}$$

Thus:

$$P = p A \tag{8}$$

where

λ is the wave length of the received noise,

D is the antenna directivity.

Substituting equation (6) and (7) into (8) gives:

$$P = \frac{D}{4H^2} V^2 \frac{\lambda^2}{480 \pi^2} \tag{9}$$

The term (10 log $\frac{D}{4H^2}$) is defined as the antenna factor and usually, for a given antenna, a graph of the antenna factors (AF) versus frequency is available with the manual of that particular antenna. For the monopole rod antenna which is used in this study, the antenna factors are given in Figure 1.

Equation (9) can be rewritten as:

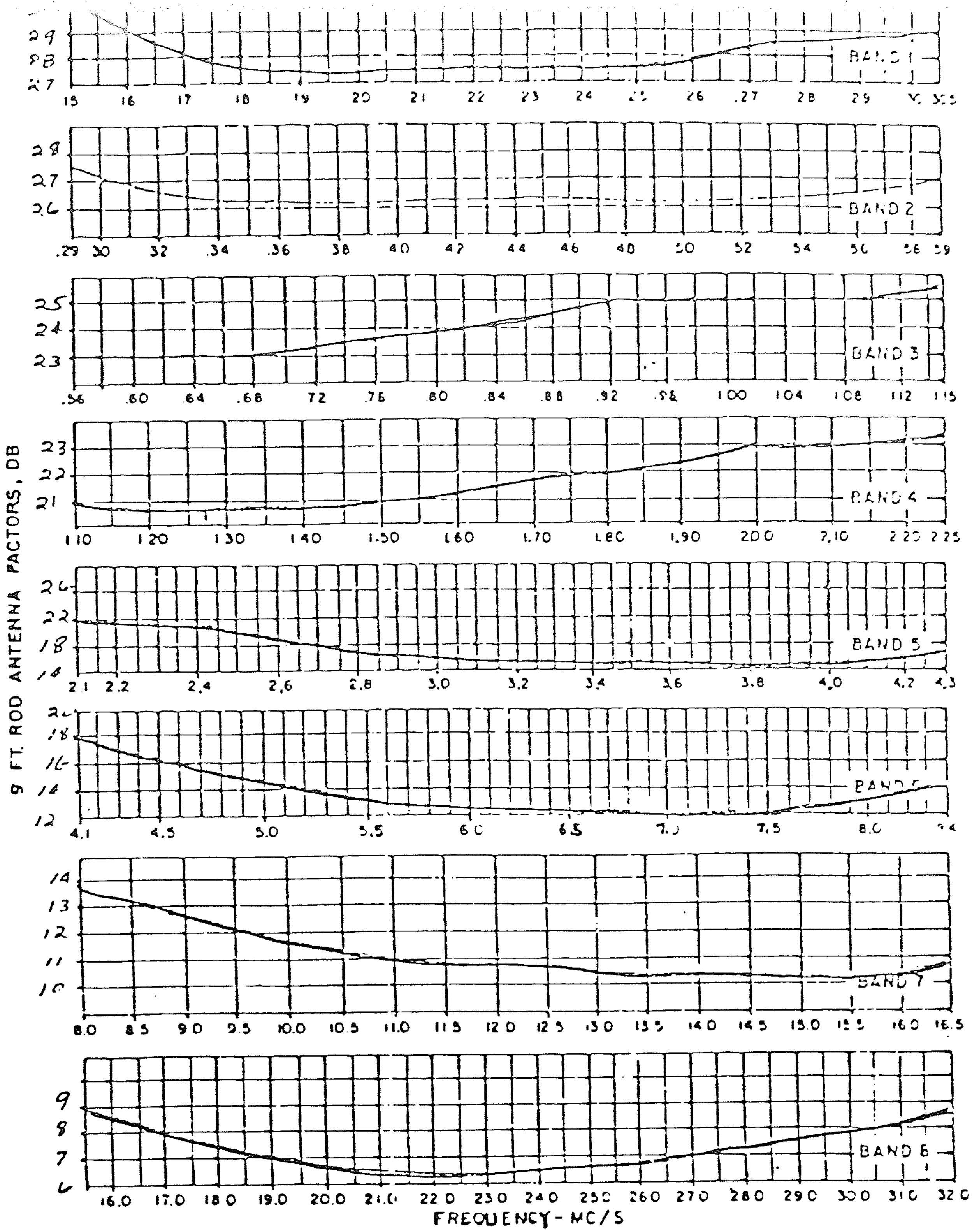

CALIBRATED BY: ______________________ 93049-1 ROD ANTENNA

DATE: ______________ SERIAL NO. SAMPLE ONLY

Note: Subtract ·2 dB to obtain field strength antenna factor.

Copied from Single 9 foot rod antenna manual

Figure (1)

Antenna factors for the nine foot long rod antenna.

$$P\ (dBW) = V(dBuV) + AF - 20\ \log f - 107.2 \qquad (10)$$

Substituting (10) into (3), we get:

$$F_a = V(dBuV) - 20\ \log f(MHz) - B(dBHz) + AF + 96.8. \qquad (11)$$

As seen from equation (11), F_a is obtained as a function of the measured noise voltage and the frequency for a given noise bandwidth.

2.3 THE VOLTAGE DEVIATION

The voltage deviation is defined as the dB difference between the rms and average noise envelope voltages. The voltage deviation, V_d , is used to identify the different types of noise amplitude distributions. Table 1 shows the classification of noise according to V_d as defined in C.C.I.R. Doc. 322 [20]. The voltage deviation is given by the equation:

$$V_d\ (dB) = 10\ \log\ (V_{rms})^2 - 20\ \log\ (V_{average}) \quad . \qquad (12)$$

2.4 SET NOISE

The term set noise is given to the internal noise of the detector meter. If the level of the power line noise to be detected is lower than that of the set noise, the detector meter will display the set noise. In other words near or below the level of set noise, power line noise cannot be detected. The set noise is obtained with respect to a reference temperature and is defined as:

$$f_s = \frac{T_e}{T_R} \qquad (13)$$

where

T_e is the effective temperature of the detector meter,

T_R is the reference temperature (288° K).

$$T_e = (f - 1)\ T_R$$

where f is the noise figure of the detector meter (11.7 dB for the NM 26T).

V_d (dB)	Type of noise distribution
1.05	Rayleigh
1.1	Gaussian
1.1 to 20	Impulsive

Table (1)

Classification of noise according to the voltage deviation, V_d

Thus,

$$F_s \text{ (dB)} = 10 \log (f - 1) T_R - 10 \log T_R \quad (14)$$

$$F_s \text{ (dB)} = 10.8.$$

2.5 LINEAR REGRESSION AND MODELLING CONCEPTS

Investigators in numerous countries have previously studied the problem of radio interference as a determinestic problem. Their objectives were to establish relationships for radio noise levels in terms of the dimensions of the lines [9]. The formulas they used do not entirely explain the difference between the measured noise from different lines, nor the fluctuations in level which have been obtained from a given line in the course of time. In fact, it is observed that the noise level of a line is unstable and sensitive to the surface state of the conductors [4, 9]. Furthermore, noise levels can and do vary from one visit to the other, even when the line parameters (current,voltage and power) are the same. Therefore we regard the process that produces the noise as a random process. Accordingly, radio noise can only be defined in statistical terms [20].

Power line noise is a slowly varying random process, thus predicting its value with respect to independant parameters such as frequency, lateral distance and line voltage, can be treated as if it were a statistically determinable phenomena.

Generally, if a dependent variable Y changes with a change in an independent variable X, one should be able to predict Y from X. The method with which these predictions are made, are introduced in this section. Statistical terms that are involved in the discussion are also presented.

2.5.1 The linear regression equation

In order to obtain the linear equation of the form:

$$Y = a + bx \tag{15}$$

which gives a best fit to the scatter diagram of N data points, we must determine the coefficients a and b in such a way that the data points lie as close to the line as possible [15]. The method of least squares fit is the one most used in statistics. When applying this method a line is fitted thorough the data points in such a way that the squared error between the data point and the fitted one has its smallest possible value as shown in Appendix A. The corresponding a and b coefficients are obtained in the Appendix and are found to be :

$$b = \frac{\Sigma XY - \frac{\Sigma X \, \Sigma Y}{N}}{\Sigma X^2 - \frac{(\Sigma X)^2}{N}} = \frac{\Sigma XY - N\bar{X}\bar{Y}}{\Sigma X^2 - N(\bar{X})^2} , \tag{16}$$

$$a = \bar{Y} - b\bar{X} . \tag{17}$$

Where

ΣX is the summation of the dependant variable,

ΣY is the summation of the independant variable,

$\bar{X}$ is the mean of the dependant variable,

$\bar{Y}$ is the mean of the independant variable.

The linear regression model is constructed with the knowledge of the slope, represented by b, and the intersection with the Y axis given by the constant coefficient a.

2.5.2 The standard error of estimate

The quantity that measures the spread of the data points around the fitted line of regression is defined as the standard error of estimate. It is a measure of how well the line of regression fits the data points. The smaller the standard error, the better the regression model fits the points. The standard error is given by the equation:

$$\hat{S}_e = \sqrt{\frac{\Sigma(Y_i - Y)^2}{N}} . \tag{18}$$

2.5.3 The standard deviation

The spread of data points around their mean is defined as the standard deviation and is given by the equation:

$$\sigma = \sqrt{\overline{Y^2} - (\bar{Y})^2} \quad . \tag{19}$$

2.5.4 The correlation coefficient

The correlation coefficient, r , gives an assessment of the degree to which the line of regression fits the data points [15]. The formula for r is quite simple and is obtained by multiplying the deviations in X and Y (from their means) for all points and dividing the result by the standard deviation of X and that of Y multiplied by the total number of data points. The correlation coefficient is given by:

$$r = \frac{\Sigma(X-\bar{X})\ (Y-\bar{Y})}{N\ \sigma_X\ \sigma_Y} \tag{20}$$

or

$$r = \frac{\frac{\Sigma XY}{N} - \bar{X}\bar{Y}}{\sigma_X\ \sigma_Y} \quad .$$

The deduction of this equation from the definition is presented in Appendix A. The closer the correlation coefficient is to unity, the better the line of regression fits the data points.

2.5.5 Confidence limits

From the sets of data under study, we try to ascertain the value of the unknown parameter (F_a), that is, to estimate its value. In doing this, it is desirable to have confidence that the value obtained represents that parameter. The limits within which the parameter has 95% probability of existence are called the 95% confidence limits. These limits define an interval which contains the mean of the parameter. Accordingly, one would have an estimate of the unknown parameter within this interval.

The concept of linear regression is applied to the data base collected for V_d and F_a to obtain the desired models of the electromagnetic interference from power lines as shown in chapter four.

Chapter III

MEASUREMENT

3.1 MEASUREMENT PLANNING AND SITE SELECTION

Studies previously performed [10]-[14] and the central Canada region study [15], [16] used certain technical considerations with regard to measurement planning and site selection. These considerations are reviewed in this chapter and appropriate criteria are accordingly assigned and presented.

The purpose of measurements and analysis is to characterize the electromagnetic noise from power lines with typical operating voltages, loads and in the environment of various weather conditions. The characterization of such noise sources is well established when the power lines chosen are isolated from other sources of interference. In order to construct a statistical model that is useful for predicting noise from similar lines, several lines that have the same line voltage should be available. To observe changes with weather, load and voltage parameters, several visits should be made to the lines.

The site selection criteria are based on the above, keeping in mind that sites to be selected should be free from other sources of interference, the following criteria were developed:

1) Lines should be at least one mile (preferably three miles) from other power lines.
2) The line should be at least three miles (preferably five miles) from the distribution or generating station.
3) Two to three lines of the same voltage should be available.
4) The lines should be accessible under most weather conditions and reasonably close to Winnipeg to allow several sites to be visited on each field trip.
5) To characterize the change of noise with distance from the center of the line, we must be able to make physical profiles on a path perpendicular to the line.
6) To obtain the line voltage and load data at the time of measurements, we need lines that are monitored by Manitoba Hydro.

In the measurement of EMI radiated by power lines, it is worth recalling that a radiating source produces a near field and a far field [1]. The main difference between these two fields is their amplitude reduction with distance from the source. The near field strength decreases as the square of the distance, while the far field reduction is directly proportional to the distance. The contribution of the near field is especially significant within distances that are shorter than one wavelength of the considered frequency, while the far field dominates at considerably longer distances. In order to characterize the electromagnetic interference radiated by power lines, it is important to examine its variation with distance in both the near and far fields. The frequency at which the noise is to be detected determines the boundary between these two fields. For the range of frequencies in which the noise was detected, the wavelength of noise ranged from 31.25 to 2916.66 feet corresponding to 32 and 0.343 MHz respectively. This wavelength range enables one to detect noise in its near and far fields (depending upon the frequency used and the type of radiator source). The importance of studying the emitted noise at different lateral locations from the center of the power line, thus arised in order to obtain the relationship between noise level and distance for the lines surveyed.

3.2 ACTUAL SITES SELECTED

The sites were selected initially by satisfying as many of the criteria as possible. These sites are shown in Figure 3 and are as follows:

A.1 This site is on line CN-8 from Parkdale to Neepawa and the voltage is 115 KV.

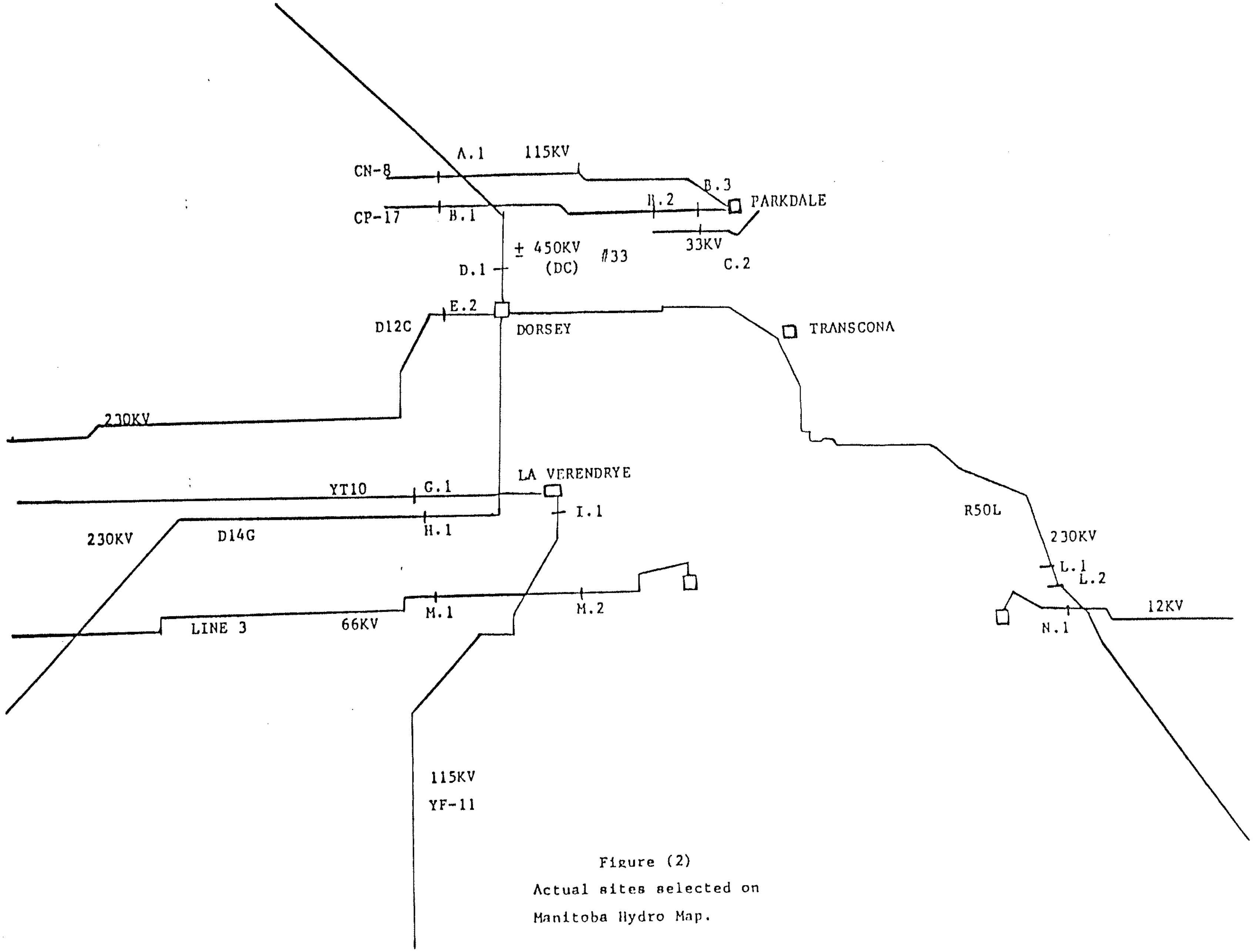

Figure (2)
Actual sites selected on
Manitoba Hydro Map.

B.1 This site is on line CP-17 from Parkdale to Portage whose voltage is 115 KV.

B.3 On the same line as B.1 but four miles from Parkdale substation.

C.2 The only 33 KV line that we found monitored by Manitoba Hydro.

D.1 This is the only site on the DC line near Winnipeg where no high voltage transmission lines run parallel to the lines. It is only three miles from Dorsey station.

E.2 This site is on line D.12C from Dorsey to Brandon and is 230 KV.

G.1 On line YT-10 which is 115 KV and is located fourteen miles west of La Verendrye station.

H.1 Located on line D14G twenty two miles from Dorsey station. It is a 230 KV line.

I.1 This site is on line YF-11 and is located three miles from La Verendrye whose voltage is 230 KV.

L.1 This site is on line R50L from Dorsey to U.S.A. and it is a 230 KV line.

L.2 On the same line as L.1, but more isolated from other electromagnetic interference sources.

M.1 This site is on line 3, which is fed from line 4 and is 66 KV. This line is energized but not loaded.

M.2 On the same line as M.1 but this portion of the line is loaded.

N.1 This site is on a labelled 12 KV line, two miles from L.2.

Each site was visited approximately ten times during the two major seasons. Frequency scans at one location, fifty feet away from the power line and lateral profiles were carried out. In Table 2, the number of lateral profiles and frequency scans performed at each site are given.

3.3 INSTRUMENTATION

The Singer NM26-T noise meter which has a noise bandwidth of 3.36 KHz was used along with a nine foot long monopole rod antenna. A coupler, model 93049-1, provided with the antenna was used to impedance match the antenna to the meter. Measurements over the frequency range of 0.3 MHz to 32 MHz were taken. The meter provides readings of rms noise voltage in dB referred to one μ V (V_{rms} dB μ V) and the voltage deviation in dB of the noise signal.

The Singer NM26T has a built-in generator for V_{rms} and V_d calibration. Calibration was performed at each test frequency before a reading was taken. According to the manual V_{rms} was calibrated to 10 dB ± 0.5dB and V_d was calibrated to 7 dB.

Man. Hydro voltage and lable	Code	Frequency* scan	Profile**
115 KV, CN-8	A.1	9	2
115 KV, CP-17	B.3	9	1
33 KV, line 33	C.2	10	0
±450 KV, bipole 1	D.1	8	2
230 KV, D12C	E.2	9	1
115 KV, YT-10	G.1	9	1
230 KV, D14G	H.1	10	1
115 KV, YF-11	I.1	9	1
230 KV, Y51L	K.1	6	1
230 KV, R50L	L.1	10	0
230 KV, R50L	L.2	8	2
66 KV, line 3	M.1	5	3
66 KV, line 3	M.2	7	2
12 KV, unlabled	N.1	7	3

* Frequency scan: The van is located at 50 feet away from the center of the line and measurements are taken for the nine test frequencies.

** Profile: The frequency is fixed and the van is moved from one location to the other to take measurements at that frequency and at different locations. After taking measurements at the five locations, the frequency is changed and the procedure is repeated at the new frequency for all locations.

Table (2)

List of profiles and frequency scans made at all sites

3.4 MEASUREMENT PROCEDURE.

The measurement procedure used in the power line noise study by Herak and Kirk [14] was considered in the early phases of this work. Herak and Kirk took ten measurements each of the rms noise voltage, the quasi-peak and the field intensity at intervals of fifteen seconds, at each of the frequencies they used . This is necessary when power line noise is measured in the presence of other electromagnetic sources such as radiation from industrial and commercial electric equipments, car ignition noise as well as from other power lines. They, as well as, Lauber and Bertrand [10], took measurements at a location fifty feet lateraly away from the power line. Since sites were selected in this study so that interference from other sources is minimized, Herak and Kirk's method of measurements was not necessary. As a measurement station we used a van, equipped with a mobile telephone through which power line data and weather information were collected. The nine foot rod antenna was mounted on top of the van and connected to the Singer noise meter.

The perpendicular distance from the center of the line was measured with the help of a survey chain and marks were placed on the road where profile measurements were to be performed, specifically at 50, 100, 150, 300 and 500 feet. Preliminary noise measurements were made to assist in deciding at which sites only frequency scans at the single location of 50 feet would be done or whether full profiles were to be performed. The main factors that motivated the performance of profile measurements were the high noise levels detected at certain sites and to characterize the noie variation with distance.

When performing a profile measurement, the van was moved to a position such that the antenna, mounted at the roof, was located at the road mark. In this way, the antenna was placed at the desired location.

Upon arrival at each site the audible noise, weather, ground conditions and power line data were obtained. These data were obtained by means of a mobile telephone. Figure 3 shows a sample data sheet of the measurements taken at the nine tests frequencies, namely 0.343, 0.49, 0.88, 1.8, 3.4, 5.6, 10.03, 18.65 and 31.62 MHz. These frequencies were chosen to be uniformly spaced on a logarithmic plot. At each frequency, measurements of V_{rms} and V_d were taken after the meter calibration procedure was performed.

Repeated visits to a particular power line indicated that the levels of the received noise changed with variations in the line voltage. A sample line was chosen and data collected, in order to characterize these changes.

SITE LABEL M2

VISIT NUMBER 4

YR 79 MO 3 DY 2

PARA.	NOISE CODES
$V_{r.m.s}$	V_d

OPERATOR M. T. Gad

FREQUENCY \ LOCATION	1 Code	1 $V_{r.m.s}$	1 V_d	2 Code	2 $V_{r.m.s}$	2 V_d	3 Code	3 $V_{r.m.s}$	3 V_d	4 Code	4 $V_{r.m.s}$	4 V_d	5 Code	5 $V_{r.m.s}$	5 V_d
0.343	2 (1.4)	14.8	2.8	2	7.3	1.9	1	24.1	1.1	1	22.1	0.9	1	21.0	0.3
0.49	2	12.9	3.0	2	6.2	2.9	1	24.0	2.0	1	24.9	2.3	1	17.5	1.8
0.88	1	26.0	1.1	1	18.3	1.1	1	16.1	0.9	1	18.9	1.1	1	14.8	1.0
1.8	2	16.2	2.8	2	7.8	1.8	2	7.3	1.7	1	19.6	0.9	1	19.5	0.4
3.4	2	14.1	2.6	2	9.8	2.7	2	13.9	3.8	2	15.7	4.9	1	17.5	2.5
5.6	2	8.9	2.1	2	6.1	2.5	2	3.2	2.1	1	17.5	1.1	1	13.7	1.8
10.03	1	23.1	1.2	1	21.0	3.0	1	19.2	1.0	1	15.2	1.3	1	12.3	1.9
18.65	1	27.8	2.0	1	22.2	2.8	1	19.2	1.9	1	13.2	1.9	1	14.9	1.8
31.62	1	14.9	1.8	1	8.1	0.8	1	9.1	1.2	1	4.9	0.9	1	4.5	1.0

Atten. setting	-20	0	20	40
Code	1	2	3	4

Noise Code

1	2	3	4
HUM	CRACKLE	SWISH	POPS

Figure (3)

Sample Data Sheet

Chapter IV

DATA PROCESSING AND RESULTS OF THE RI PREDICTIONS FOR THE SURVEYED POWER LINES.

4.1 INTRODUCTION

In this chapter, the computer processing of measured data obtained from the field trips is presented, in order to obtain estimates of the radio interference from the surveyed power lines. In the procedure, the linear regression technique is applied through computer programs to produce relations that model the radio interference. These relations are:

1) Relation between the effective antenna noise factor (F_a) and the frequency (f).
2) Relation between F_a and the lateral distance from the center of the line.
3) Relation between F_a and line voltage.
4) Relation between the voltage deviation (V_d) and f.

The method and sequence of processing the data as well as the computer programs used to obtain the results are presented. The noise performance of an unloaded power line and the effects of weather conditions (rain, snow and fair weather) upon the noise characteristics are also discussed in this chapter.

4.2 F_a COMPUTATION

The data base of V_{rms} and V_d collected were entered into computer files. A computer program was written to compute F_a using equation (11) derived in chapter two. In order to calculate the F_a values, various adjustments were necessary to restore the actual values of the noise signal radiated by the power line. In doing this, one has to recall that the signal attenuates at the antenna terminal, at the cable and possibly at the detector meter (depending upon the position of the attenuator control). The following example illustrates the various adjustments that are applied to V_{rms} data in order to calculate F_a.

Example of F_a calculation

Data:

Location: 50 feet from the center of the line.

Frequency: 31.62 MHz.

V_{rms} on NM26T: 26.2 dBμV.

Attenuator setting on the meter (A): -20 dB.

Antenna factor at 31.62 MHz: 26.1 - 2 = 24.1 dB.

Meter noise bandwidth: 3.36 KHz.

Calculation:

$$F_a \text{ (dB)} = 26.2 - 20 - 20 \log (31.62) - 10 \log (3360) + 24.1 + 96.8$$

F_a (dB) = 62.1

If the F_a value is lower than the set noise, the meter will display only the set noise and not the F_a level. This internal noise domination was not encountered in any of the field trips. In other words, the power line noise level was higher than that of the internal noise at least of one order of magnitud.

4.3 APPLICATION OF LINEAR REGRESSION ON F_a VALUES

Since EMI emitted from power lines is a random process, only a statistical analysis of its characteristics will yield meaningful results. The linear regression technique [15]-[17] is applied to F_a in order to construct prediction models for the various voltage classes of power lines surveyed. Using these prediction models, the noise levels from similar power lines of the same line voltage can be obtained within the specified frequency range assuming same enviromental conditions. The application of linear regression to the relationships of F_a with respect to parameters such as frequency, distance and line voltage, is presented and discussed in this section. The results of the computation of these relationships are also included in the discussion.

A utility subprogram was used to perform the linear regression and obtain the required models. The subprogram was obtained from the International, Mathematical and Statistical Library (IMSL). This program evaluates the point estimate, standard error and the lower and upper confidence limits. Calculations for the mean, standard deviation of both the intercept and the response variables, and the correlation between them were also obtained by using the subprogram. The program was applied to F_a values in order to obtain models of the noise with respect to the frequency, distance and line voltage parameters.

4.3.1 F_a versus log f relationship

The calculation of F_a given in the previous section was applied to the ten sets of V_{rms} data obtained for the ten separate visits made to each power line. This yielded an average F_a value over the ten visits at a particular test frequency. Average F_a values were determined at each site for the nine test frequencies. Linear regression was applied to these average F_a values to obtain a model such as that presented in figure (4). The figure shows the linear regression approximation of the average F_a values obtained from site B.3 (115 KV) at a location 50 feet lateraly away from its center. The correlation coefficient (which mea-

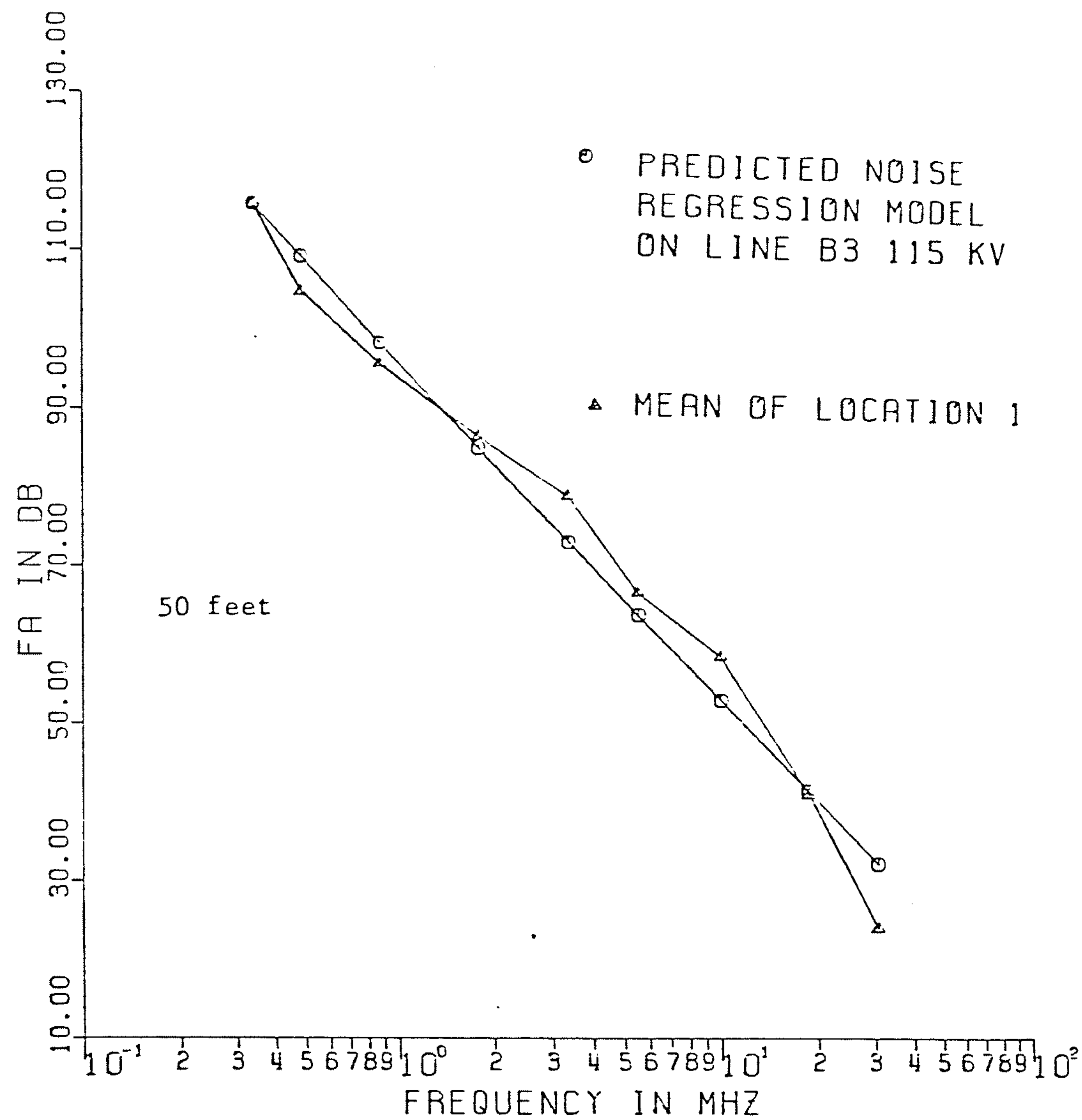

Figure (4)

Application of linear regression to the mean noise at fifty feet from the center of the line.

sures the degree to which the linear regression fits the average F_a values) is 0.99. This high correlation coefficient shows a strong dependence of F_a on frequency. The model obtained for site B.3 under normal operating conditions is as follows:

$$F_a = 92.3 - 36.5 \log f \pm 4$$

The above procedure considers F_a values obtained at the first location (50 feet) from the power line. The procedure was then repeated for the other four locations 100, 150, 300 and 500 feet. The whole process of obtaining the F_a versus log f relationship at the five test locations was applied to all transmission lines surveyed. Figures (5a-l) show F_a variation with the logarithm of frequency at the five test locations for each site, with the exception of sites C.3 (33 KV) and L.1 (230 KV), where no profile measurements were performed. The main feature of the graphs is the decrease of the F_a levels with increase in frequency. The F_a decrease with frequency at the first location as obtained from figures (5a-l) respectively, is presented in table (3)

The correlation coefficient ranged from 0.8 to 0.99 for the results given in figures (5a-l). From table (3), it is seen that the slopes of the F_a versus log f relationship decreases as the line voltage increases. This same result

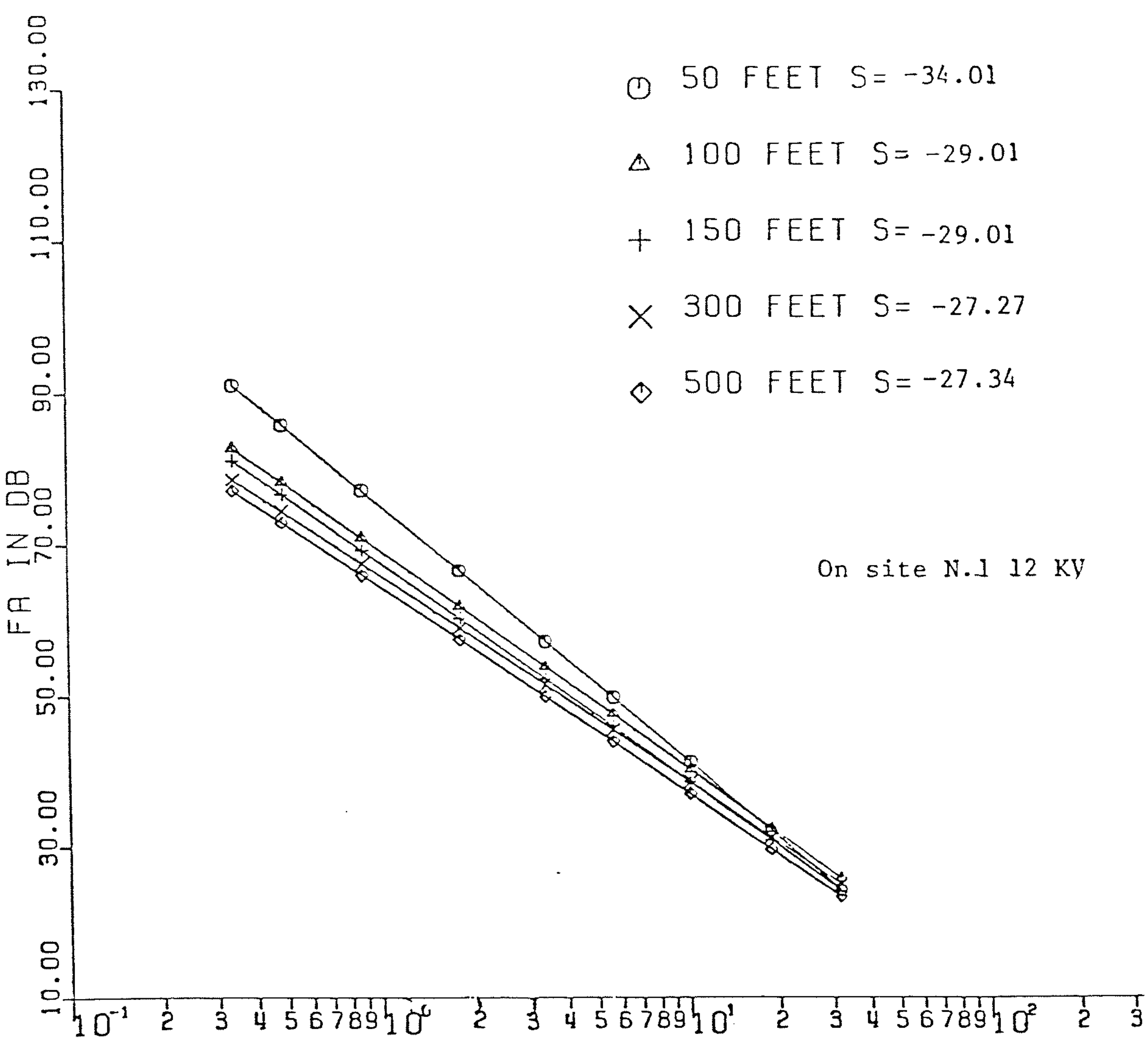

Figure (5a)

F_a variation with frequency with the distance as a parameter.

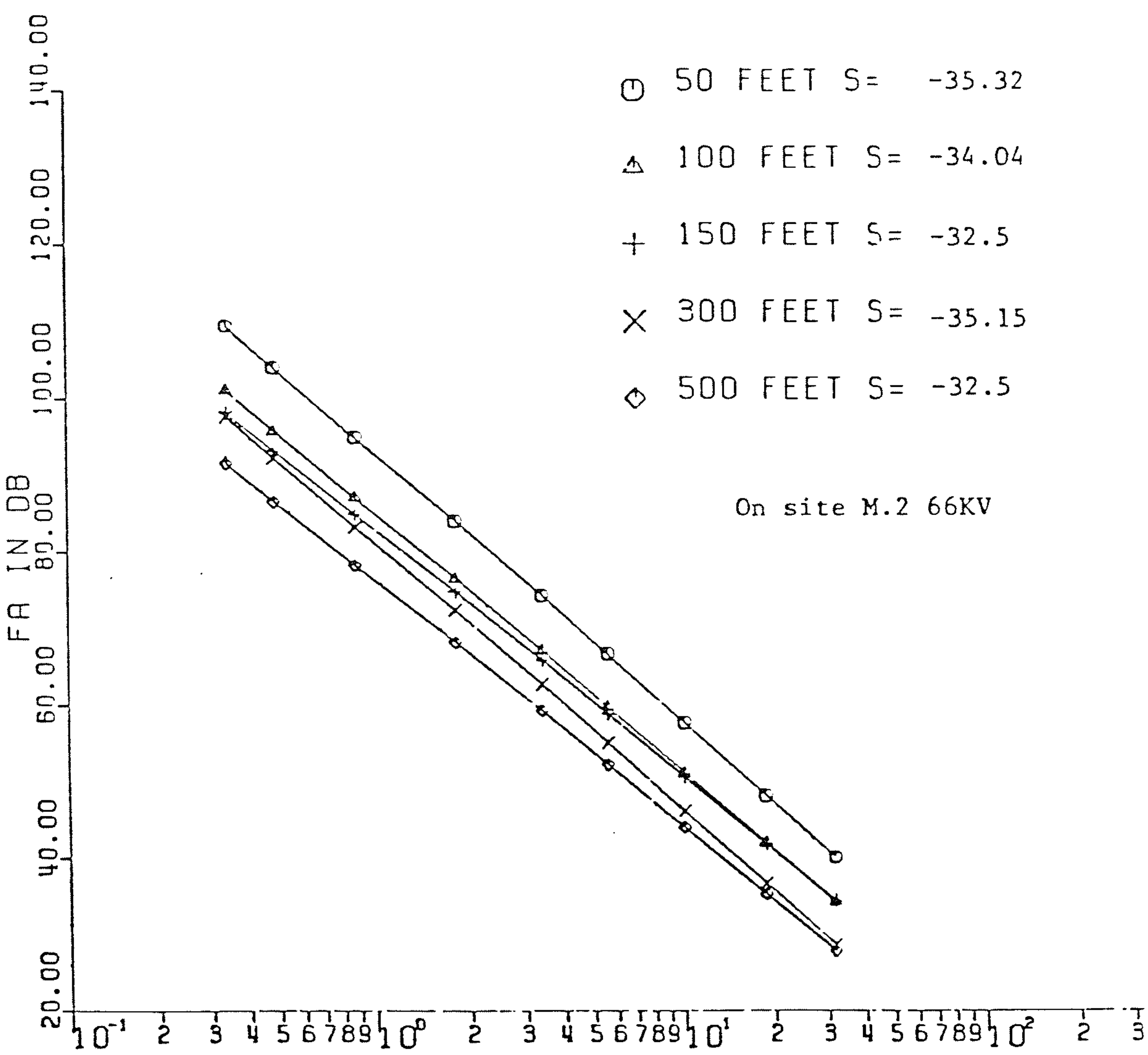

FREQUENCY IN MHZ

Figure (5b)

F_a variation with frequency with the distance as a parameter.

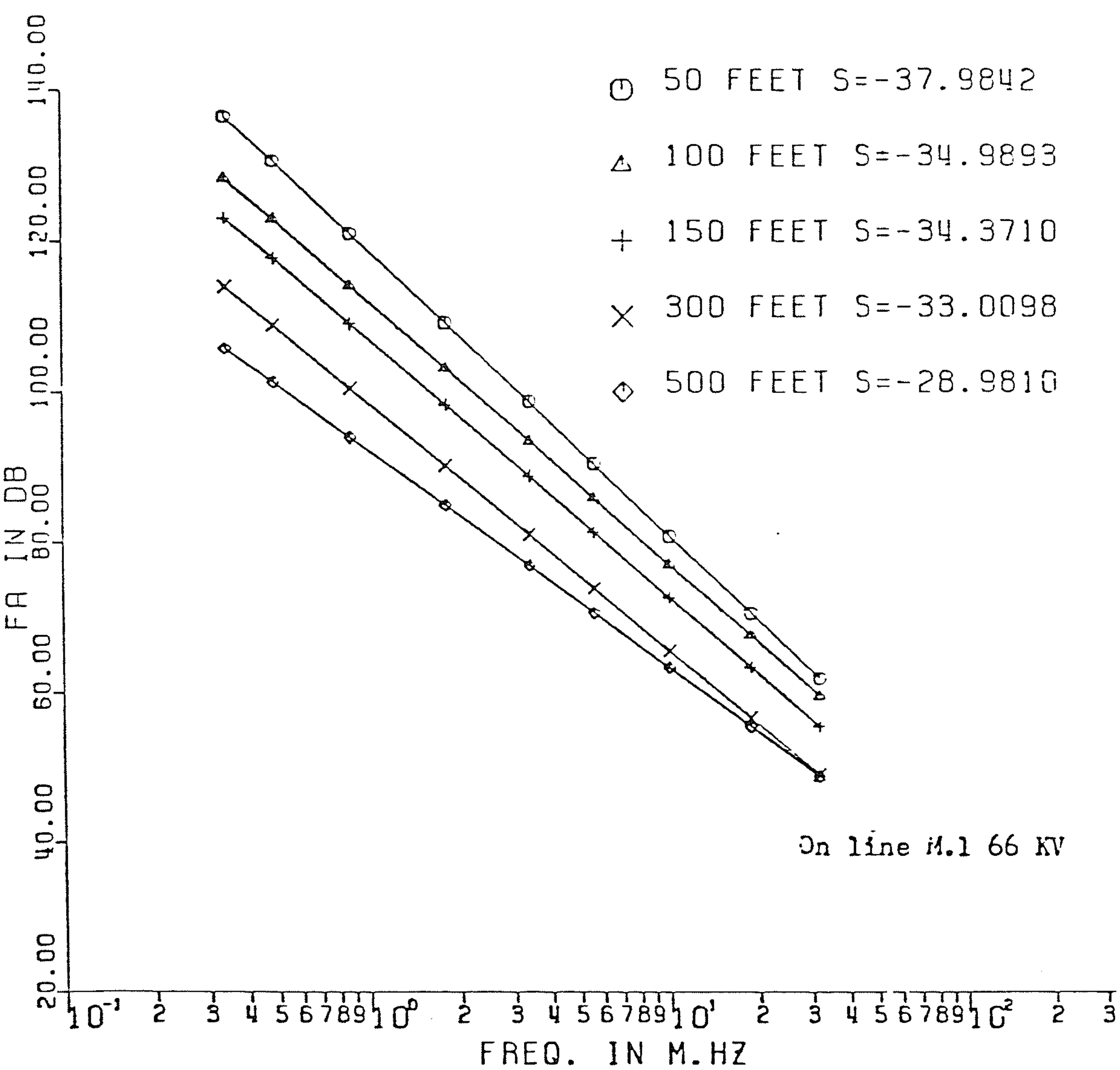

Figure (5 c)

F_a noise levels received

from the unloaded line.

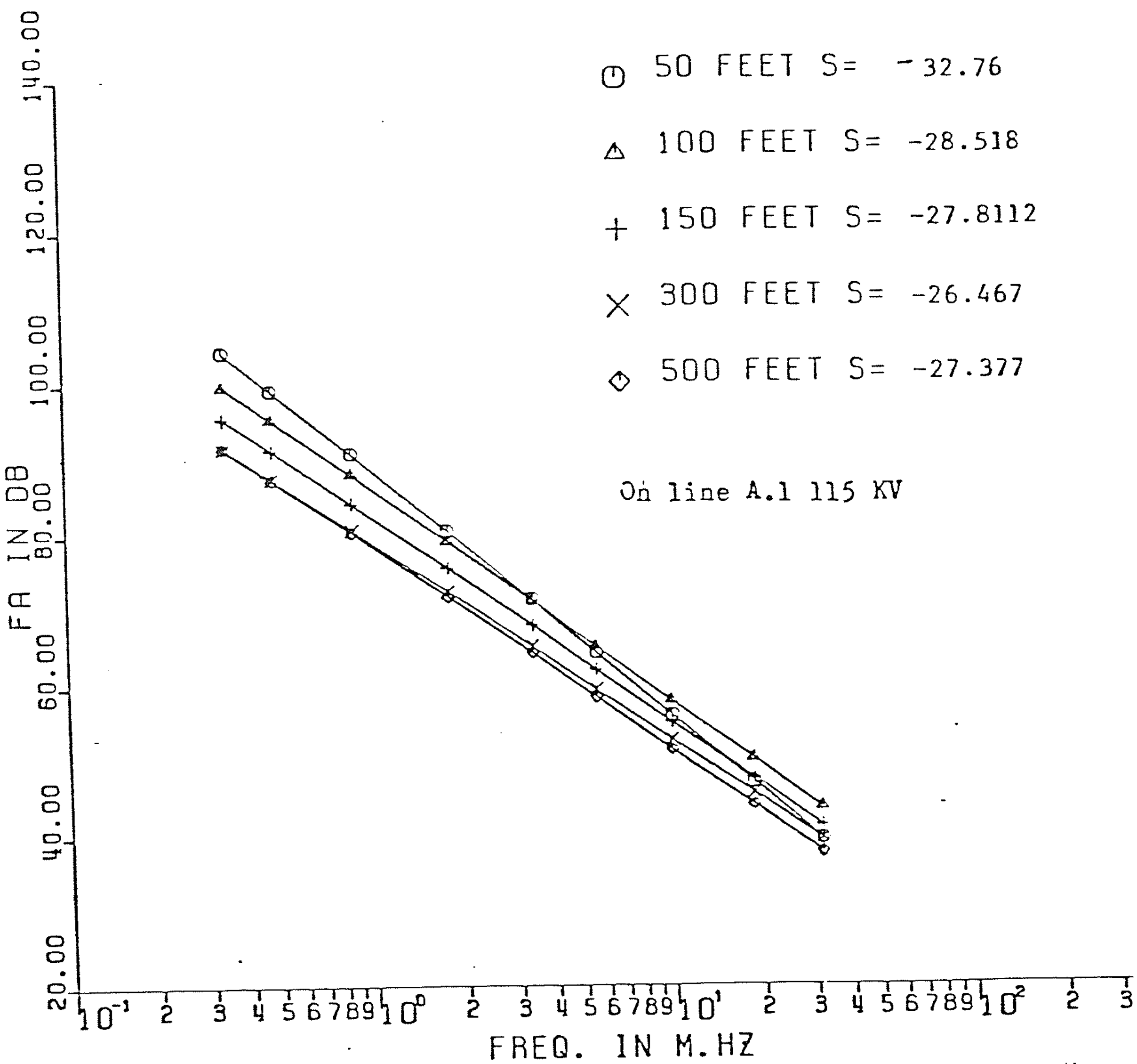

Figure (5d)

F_a versus frequency with the

distance as a parameter.

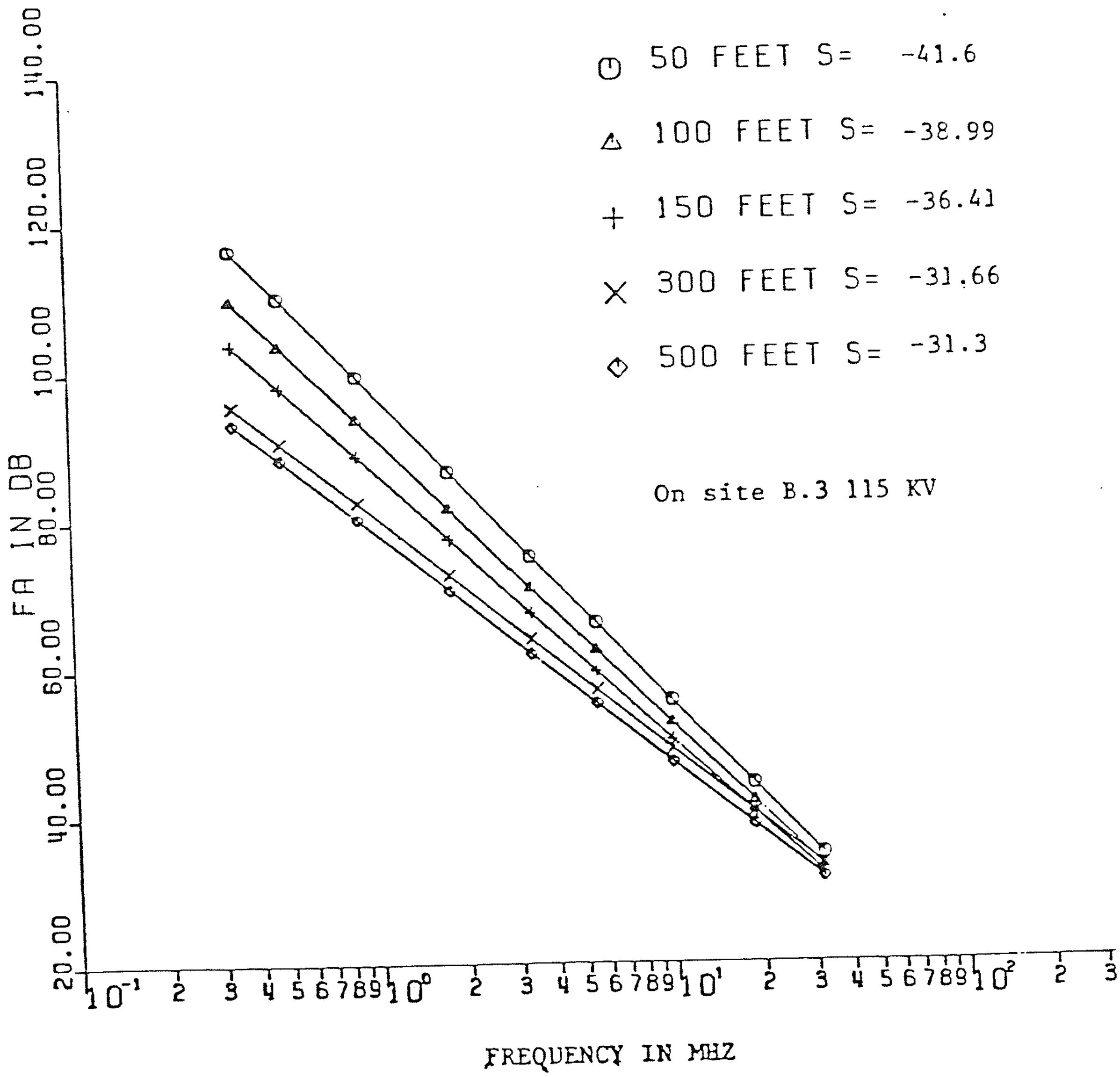

Figure (5e)

F_a versus frequency with distance as a parameter.

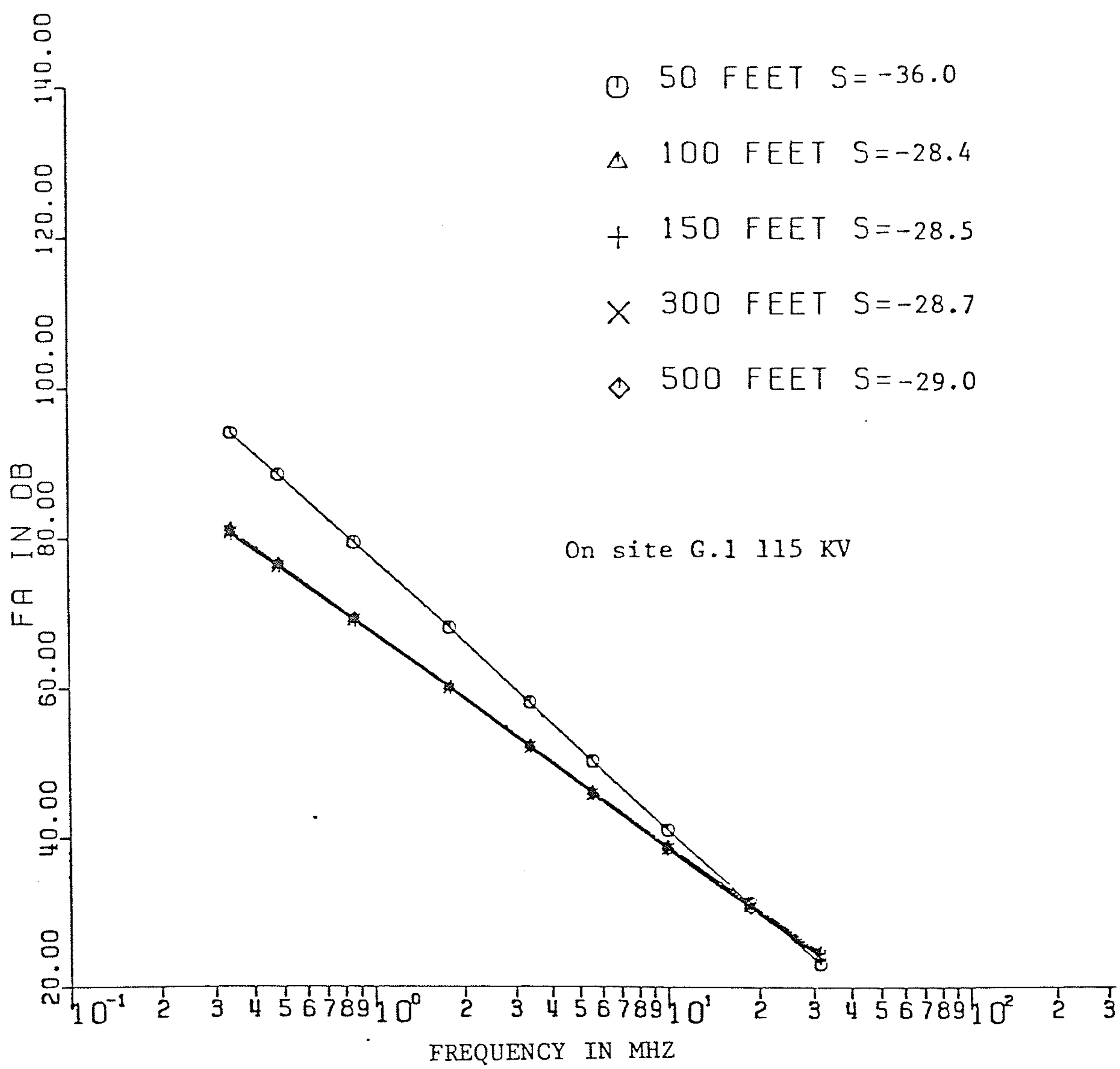

Figure (5f)

F_a variation with frequency with the distance as a parameter.

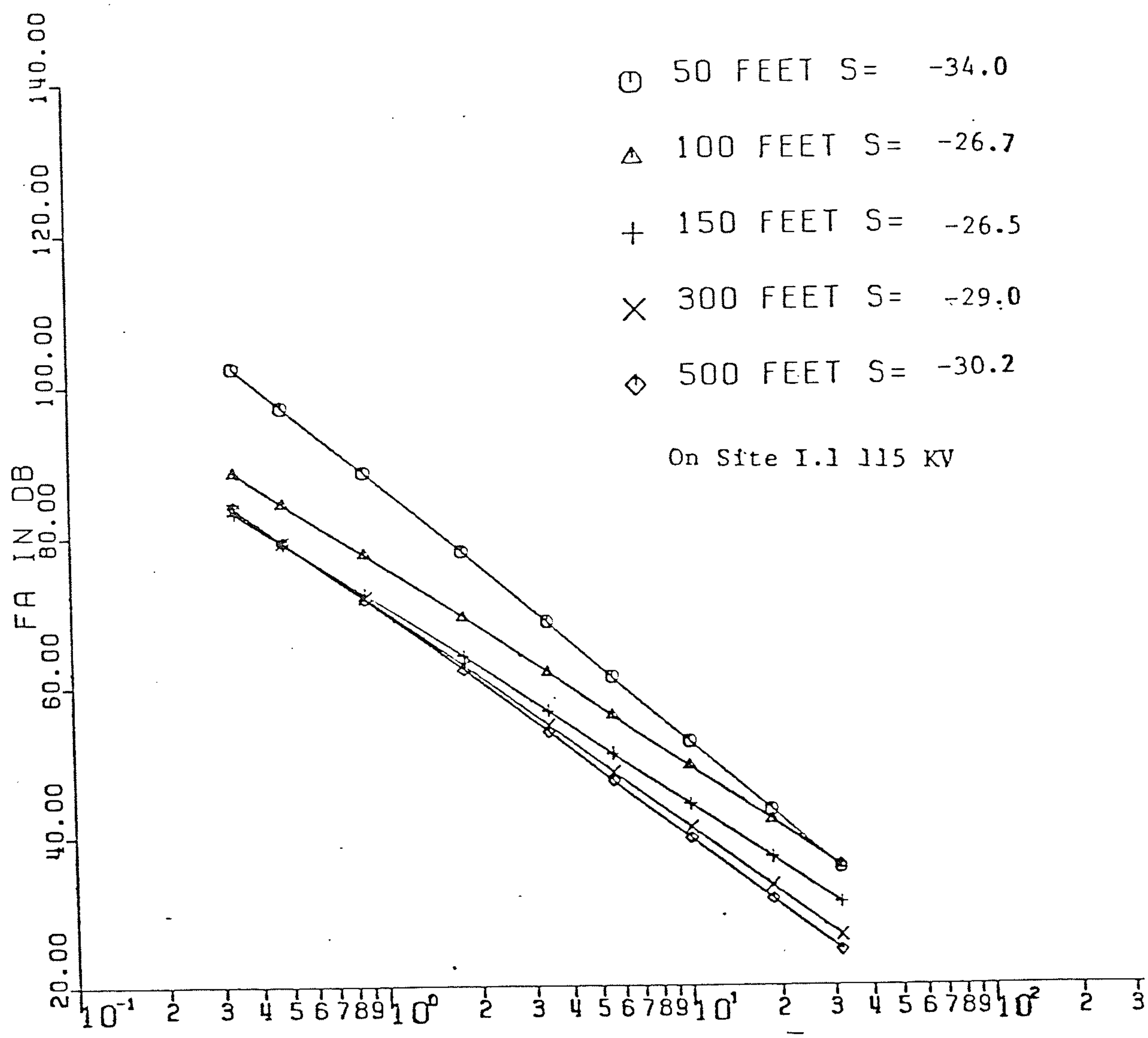

Figure (5g)

F_a versus frequency with the distance as a parameter.

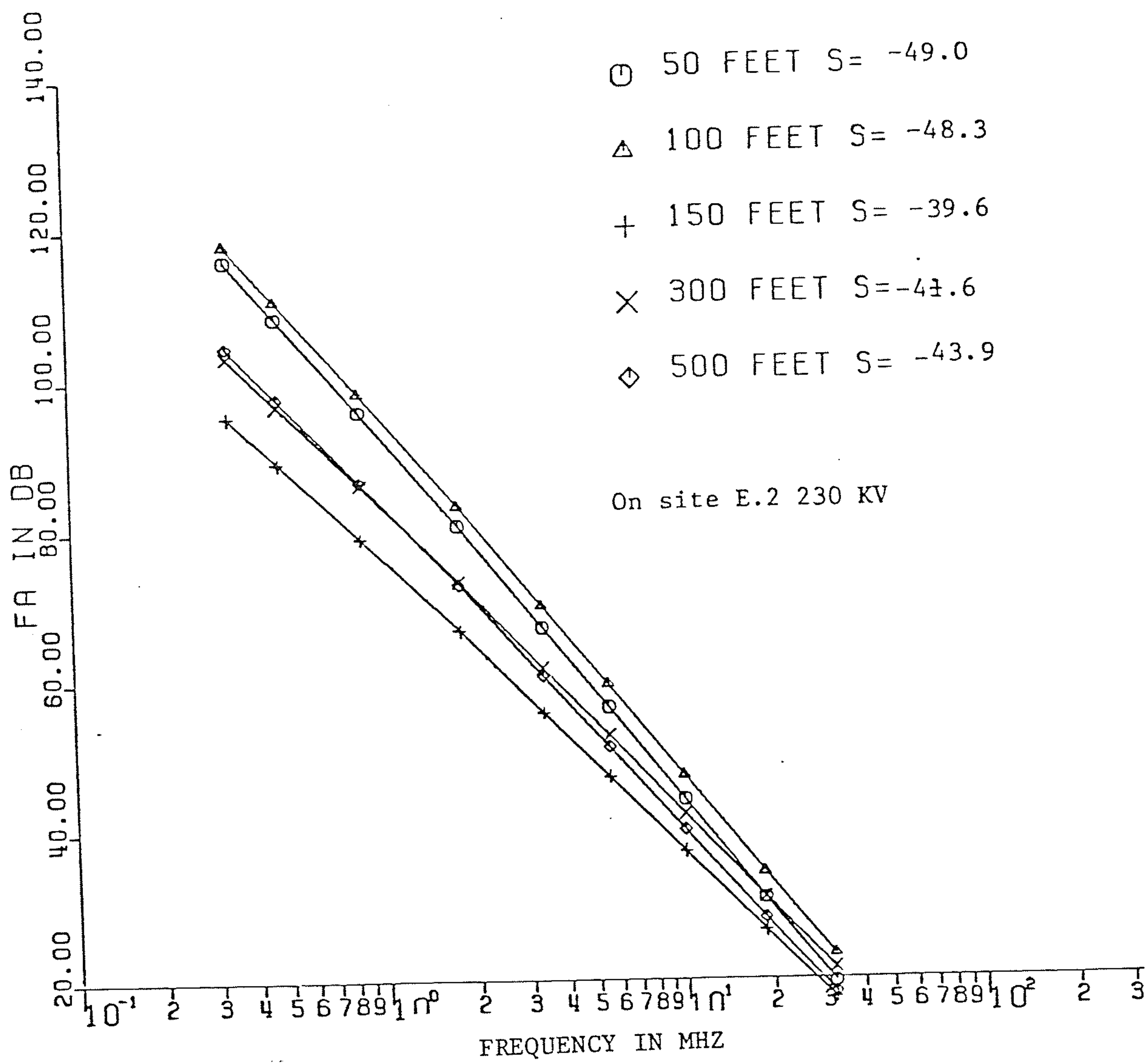

Figure (5h)

F_a variation with frequency with the distance as a parameter.

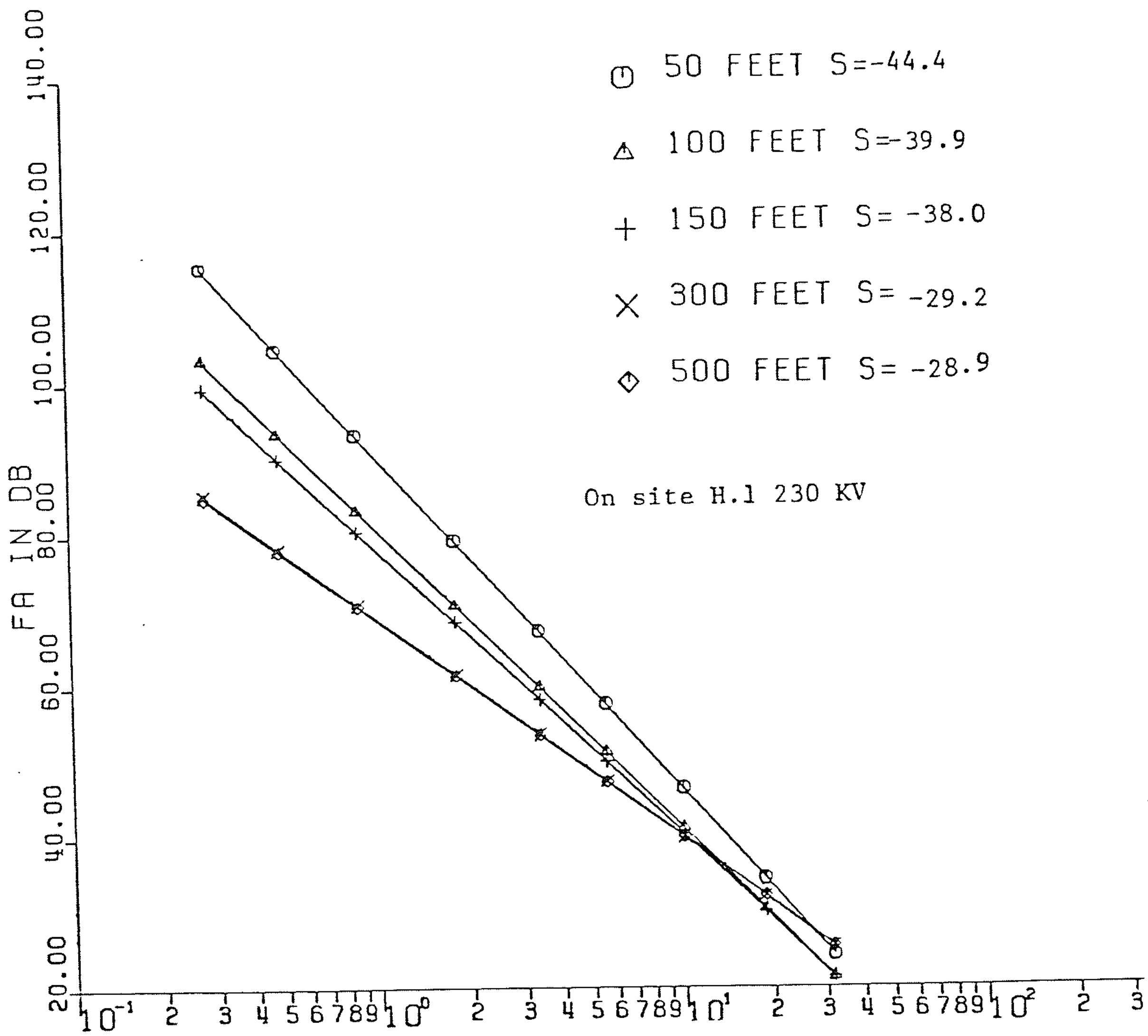

Figure (5i)

F_a variation with frequency with the distance as a parameter.

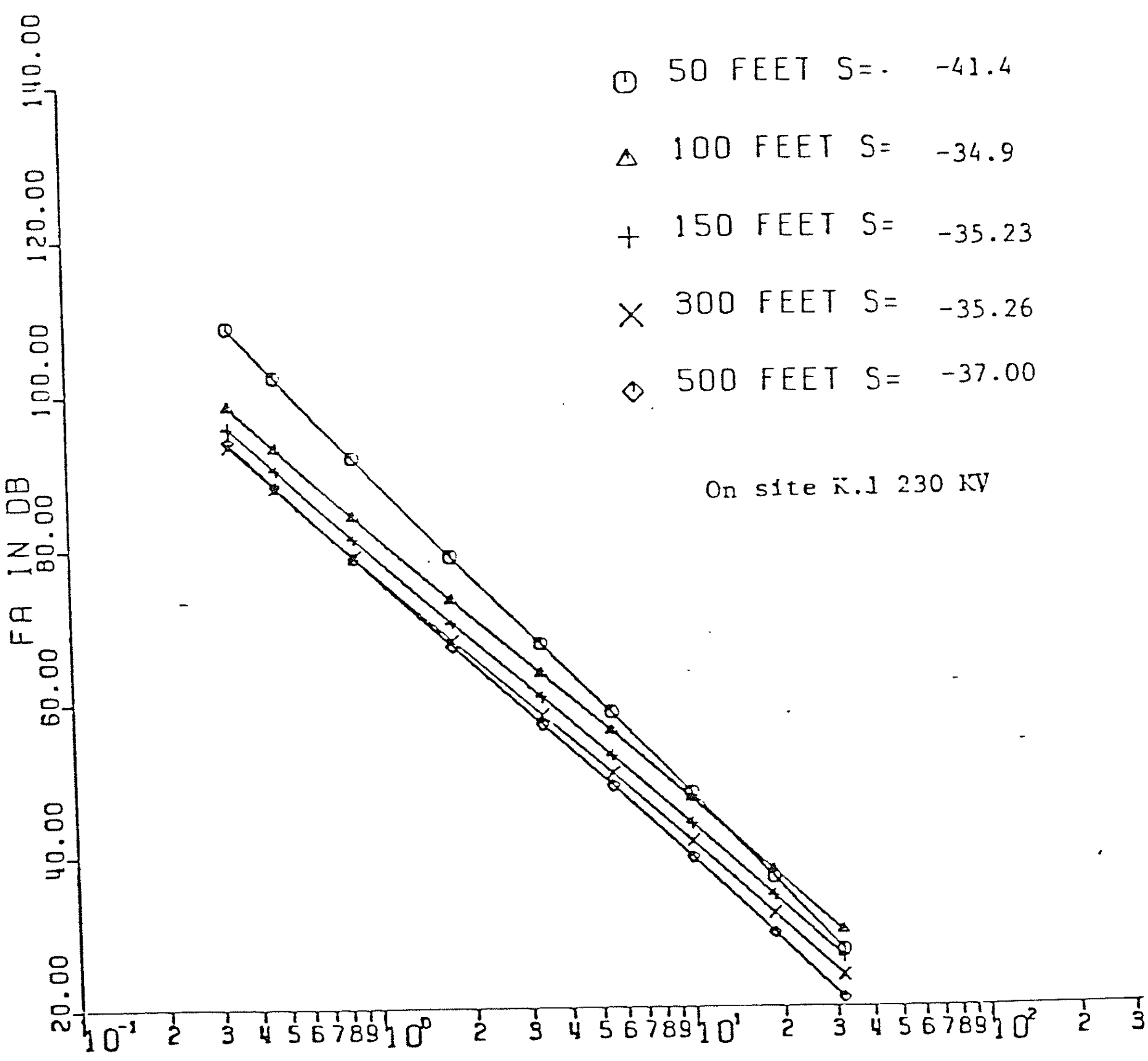

Figure (5j)

F_a versus frequency variation
with the distance as a parameter.

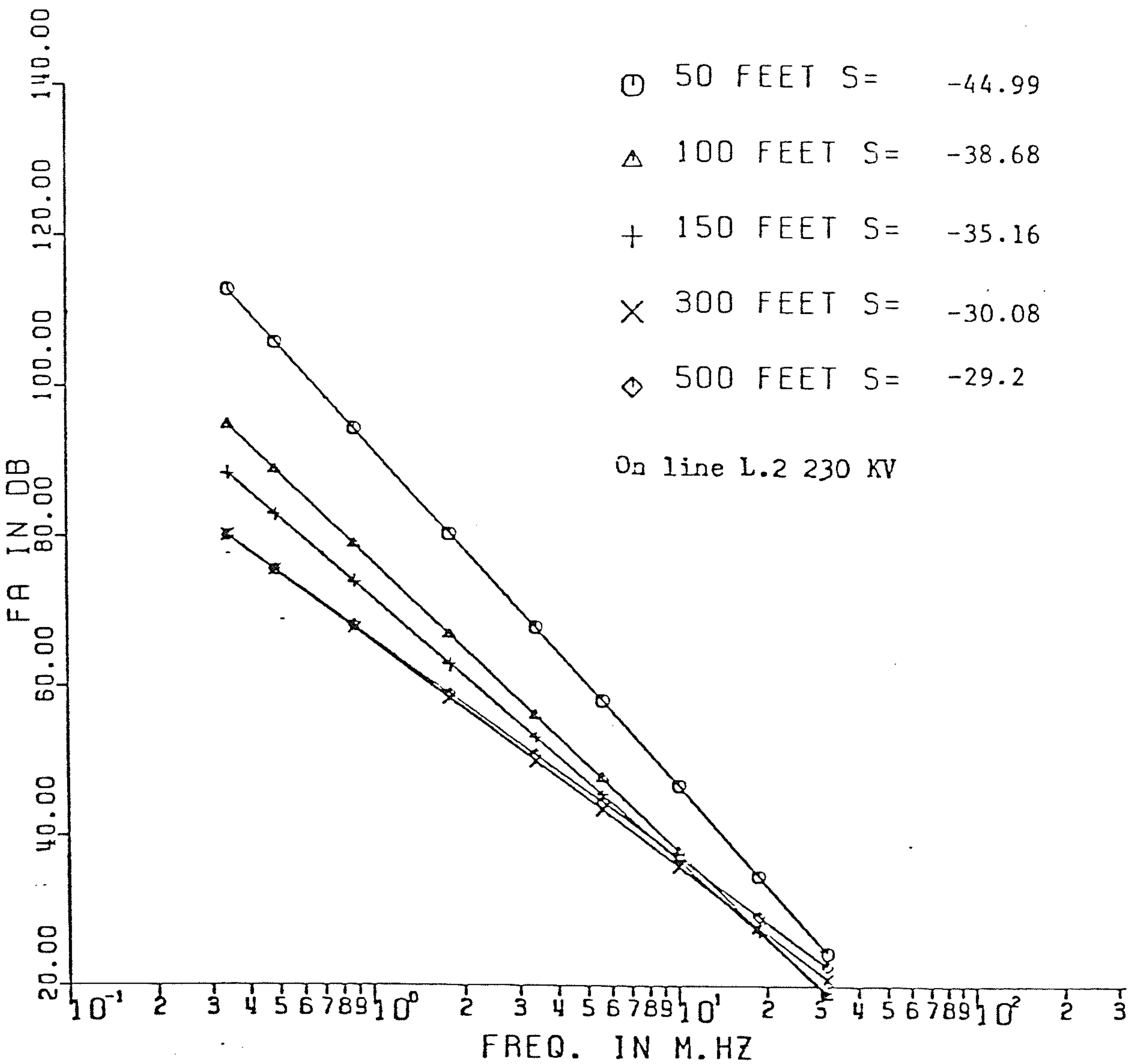

Figure (5k)

F_a versus frequency with distance as a parameter.

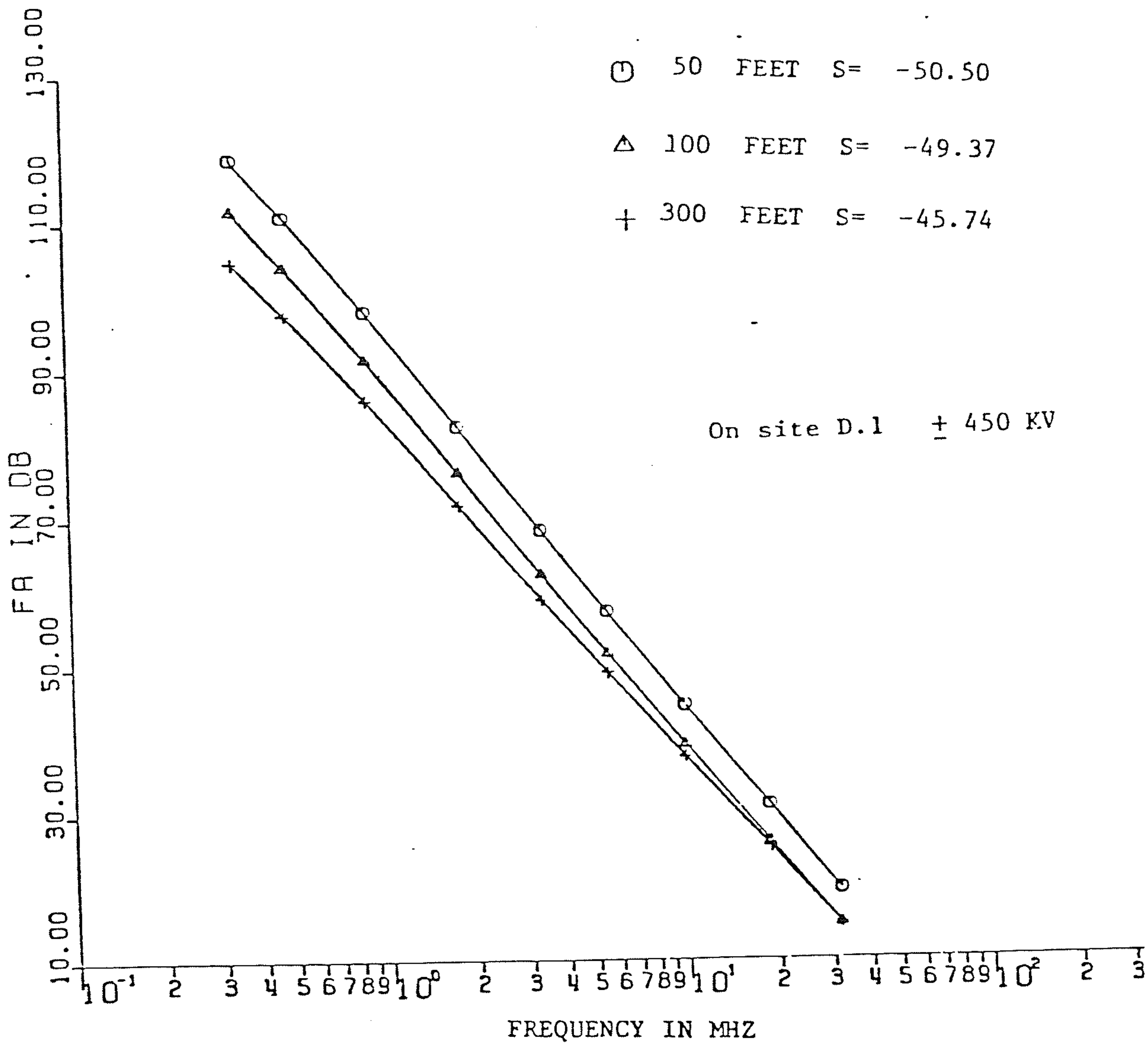

Figure (51)

F_a variation with frequency with the distance as a parameter.

Figure	Site	Voltage in KV	Slope (dB/decade)
5a	N.1	12	-34.00
5b	M.2	66	-35.32
5c	M.1	66	-37.98
5d	A.1	115	-32.76
5e	B.3	115	-41.60
5f	G.1	115	-36.00
5g	I.1	115	-34.00
5h	E.2	230	-49.00
5i	H.1	230	-44.00
5j	K.1	230	-41.40
5k	L.2	230	-44.99
5l	D.1	±450	-50.50

Table (3)

Slopes of F_a models with frequency obtained from figures (5a-l) at 50 feet.

is obtained in section 4.3.3 where the F_a versus log V relationship is determined. As seen from table (3) sites A.1 (115 KV), site I.1 (115 KV) and site G.1 (115 KV) gave slopes of -32.76, -34.0 and -36.0 dB/frequency decade, respectively, when modelled using the linear regression technique. Site B.3 (115 KV) produced an F_a model of slope -41.6 dB/frequency decade. A comparison of these slopes shows that site A.1, I.1 and G.1 produced negative slopes which were not as steep as the slope obtained for site B.3, although the four sites have the same line voltage. This may be due to the difference in line design factors (i.e., conductor radius, phase spacing and insulator type) between these lines. Deterioration of hardware components on a power line due to aging can cause greater noise emission [1,6]. This factor must also be kept in mind when looking at the slopes of the F_a characteristics.

The decrease of F_a with frequency for the other four locations can also be obtained from figures (5a-l). It is apparent that there is a greater drop in F_a levels with an increase in frequency than with an increase in distance from the power line. This can be further explained if, for example, the results in figure (5a) are examined. In the figure, the F_a value at 0.343 MHz is 92 dB while at 30.62 MHz it is 25 dB, which results in a difference of 67 dB. In the same figure, it is seen that F_a at 50 feet is 92 dB while at

500 feet F_a is 77 dB (both values are taken at the same frequency of 0.343 MHz). This gives a difference of 15 dB which is less than the difference of 67 dB obtained by increasing the frequency by a decade. The relationship between F_a and distance is investigated in the following section.

4.3.2 F_a versus log d relationship

The F_a variation with the logarithm of lateral distance from the power line was obtained using a computer program. The program applies the linear regression analysis to all F_a values obtained at a particular site at each frequency with the distance of each test location as the independent variable. The procedure was applied to the nine test frequencies. This resulted in models of F_a with respect to distance from the power line for each frequency. Although models could be obtained for all nine test frequencies, the program was adjusted so that only five models at 0.343, 0.88, 3.4, 10.03 and 30.62 MHz were plotted. Models were obtained for all lines for which profile measurement were performed. Figures (6a-l) show the F_a variation with the logarithm of distance for all power lines with the exception of site C.3 (33 KV) and site L.1 (230 KV) where no profile measurements were performed. As a general observation from the figures, it is clear that noise levels drop with

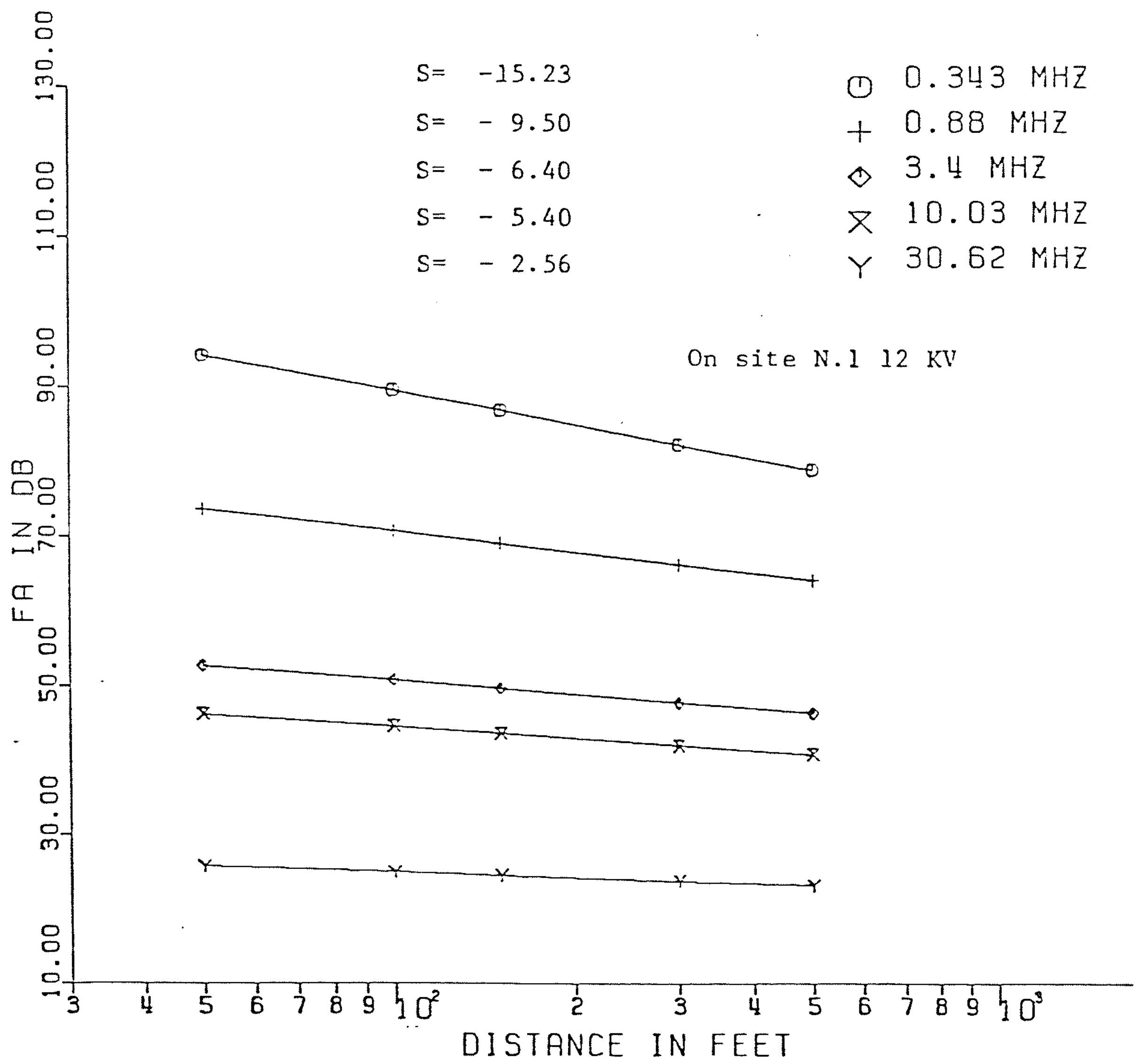

Figure (6a)

Variation of noise with distance
having the frequency as a parameter.

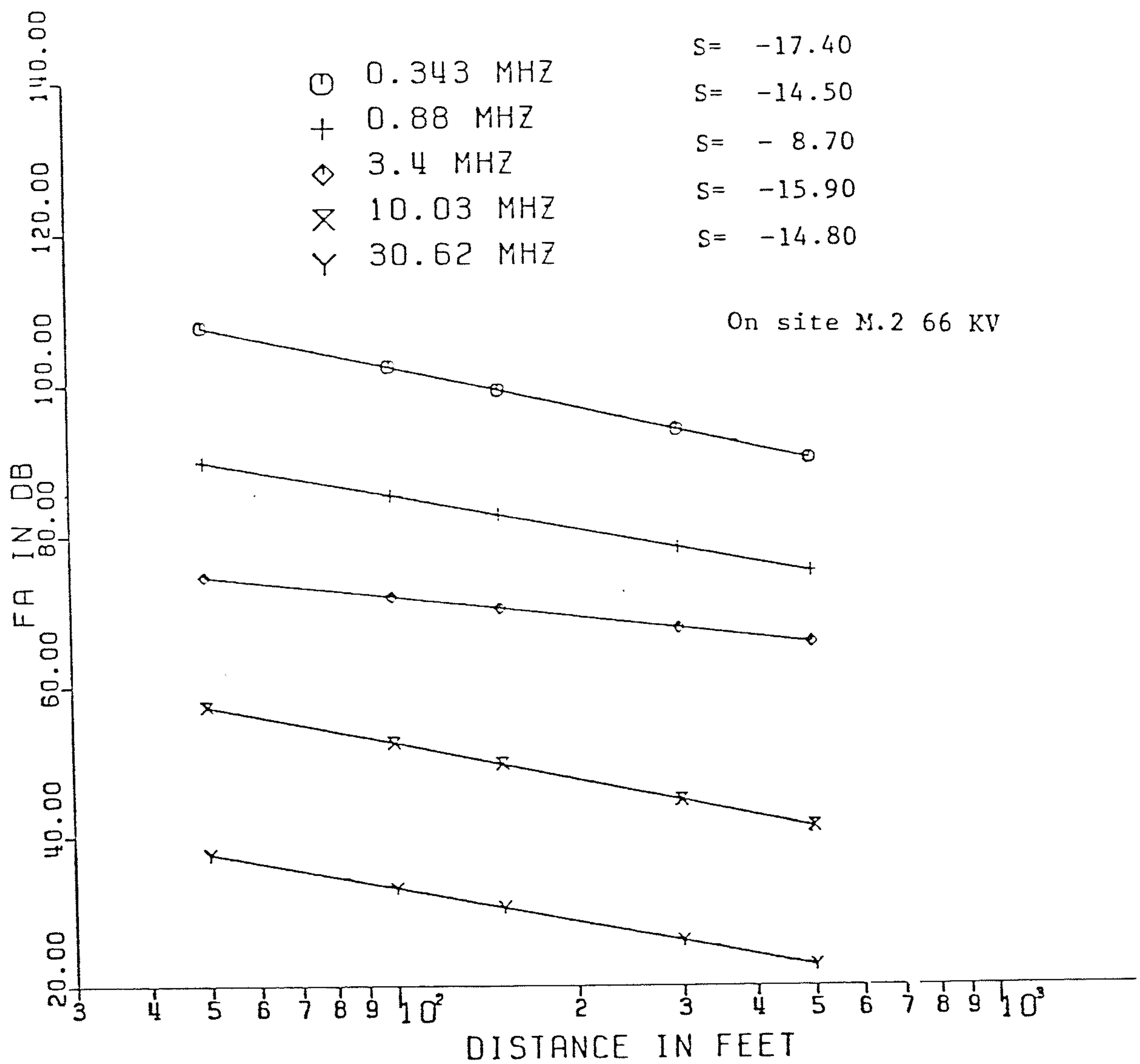

Figure (6b)

Variation of noise with distance having the frequency as a parameter.

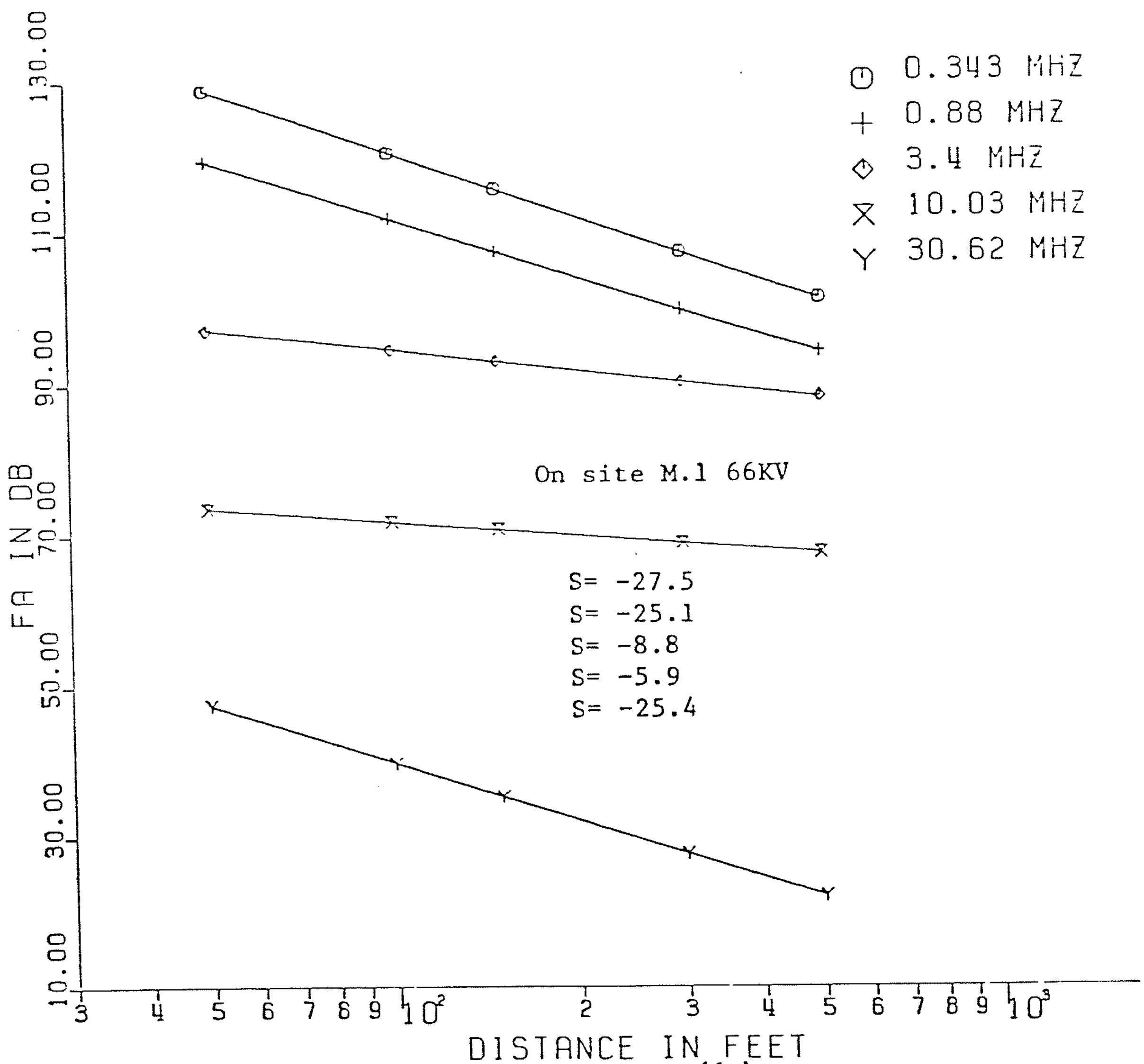

Figure (6c)
Variation of noise with distance having the frequency as a parameter.

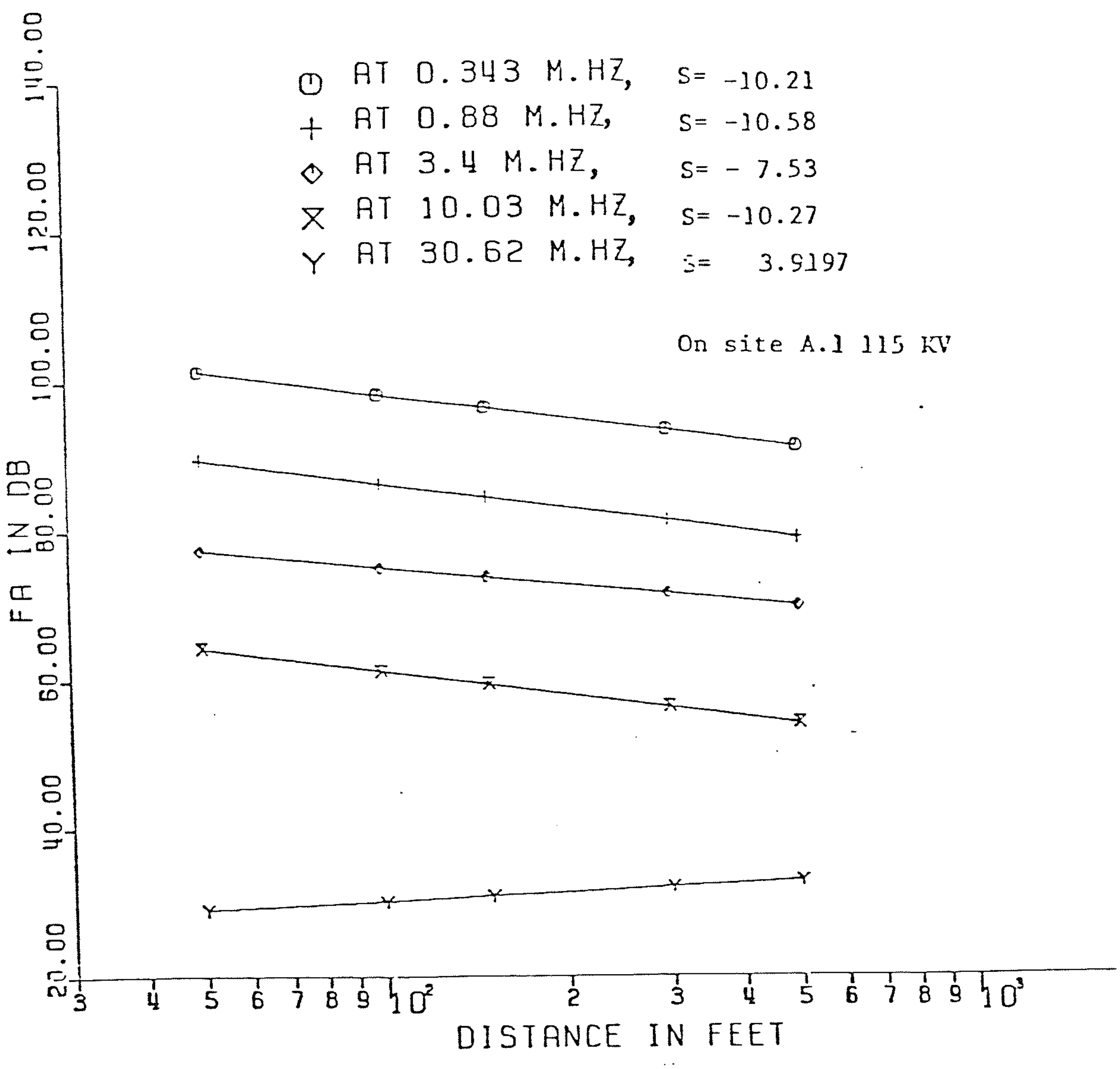

Figure (6d)

Variation of noise with distance

having the frequency as a parameter.

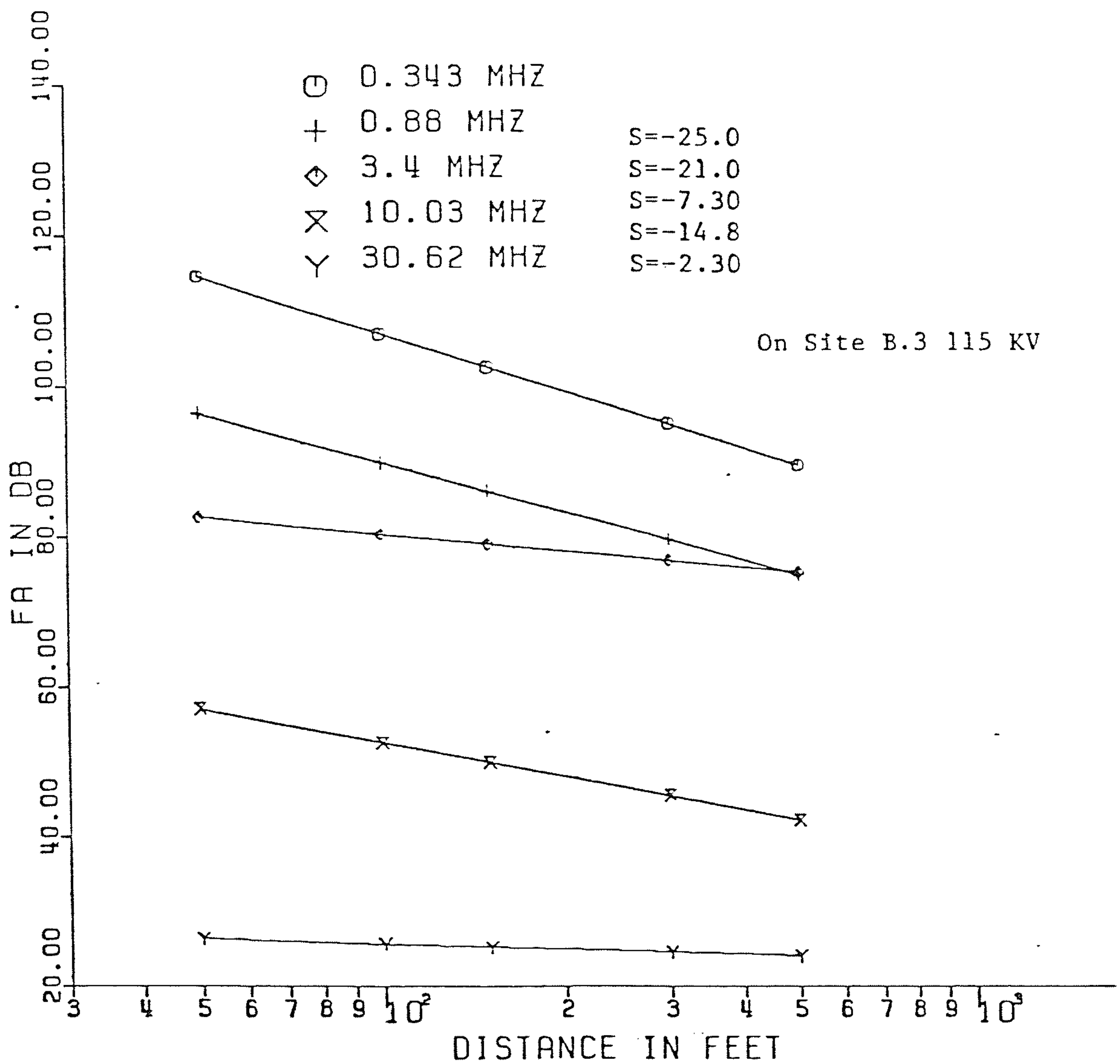

Figure (6e)

Variation of noise with distance having the frequency as a parameter.

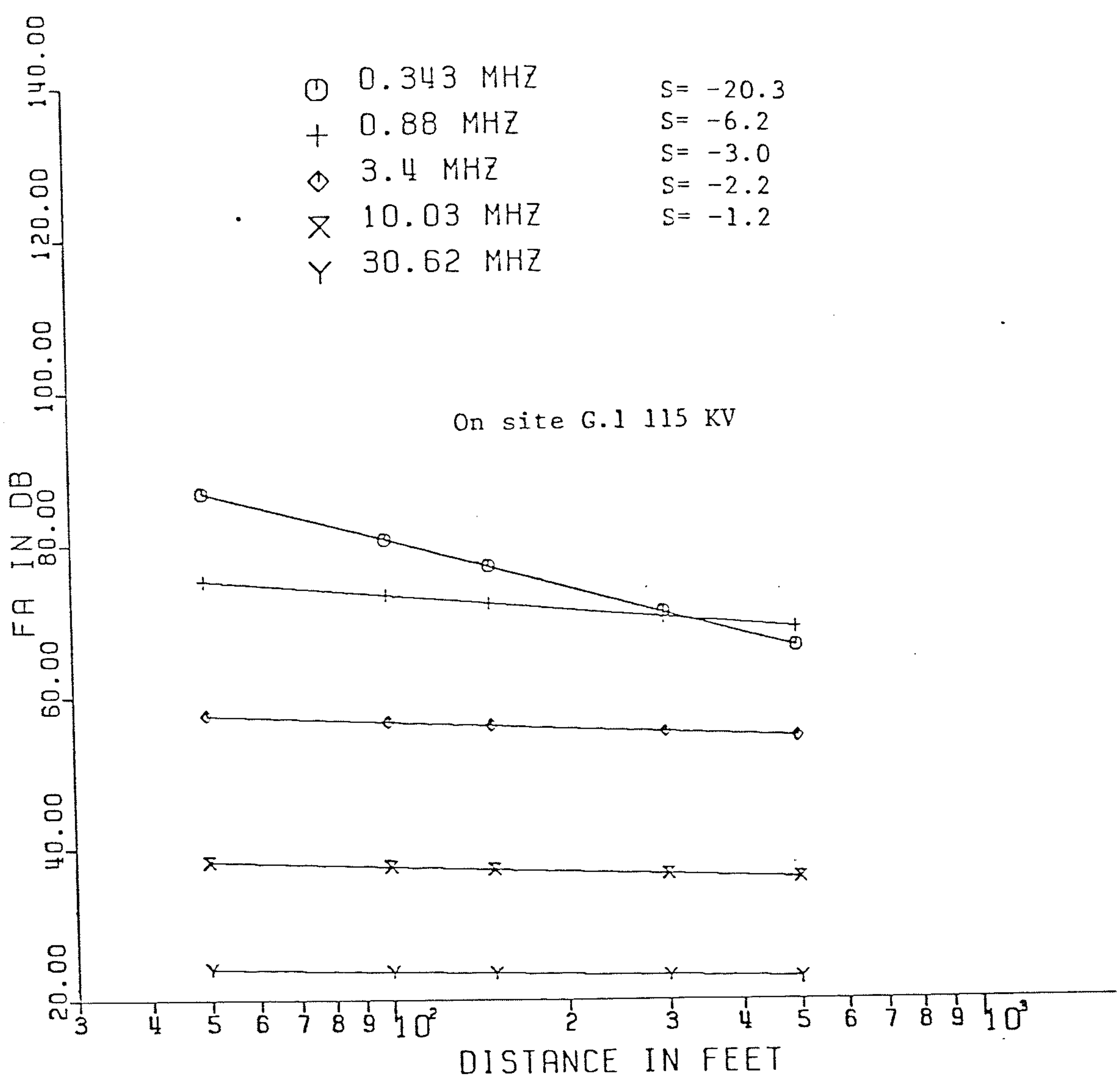

Figure (6f)

Variation of noise with distance having the frequency as aparameter.

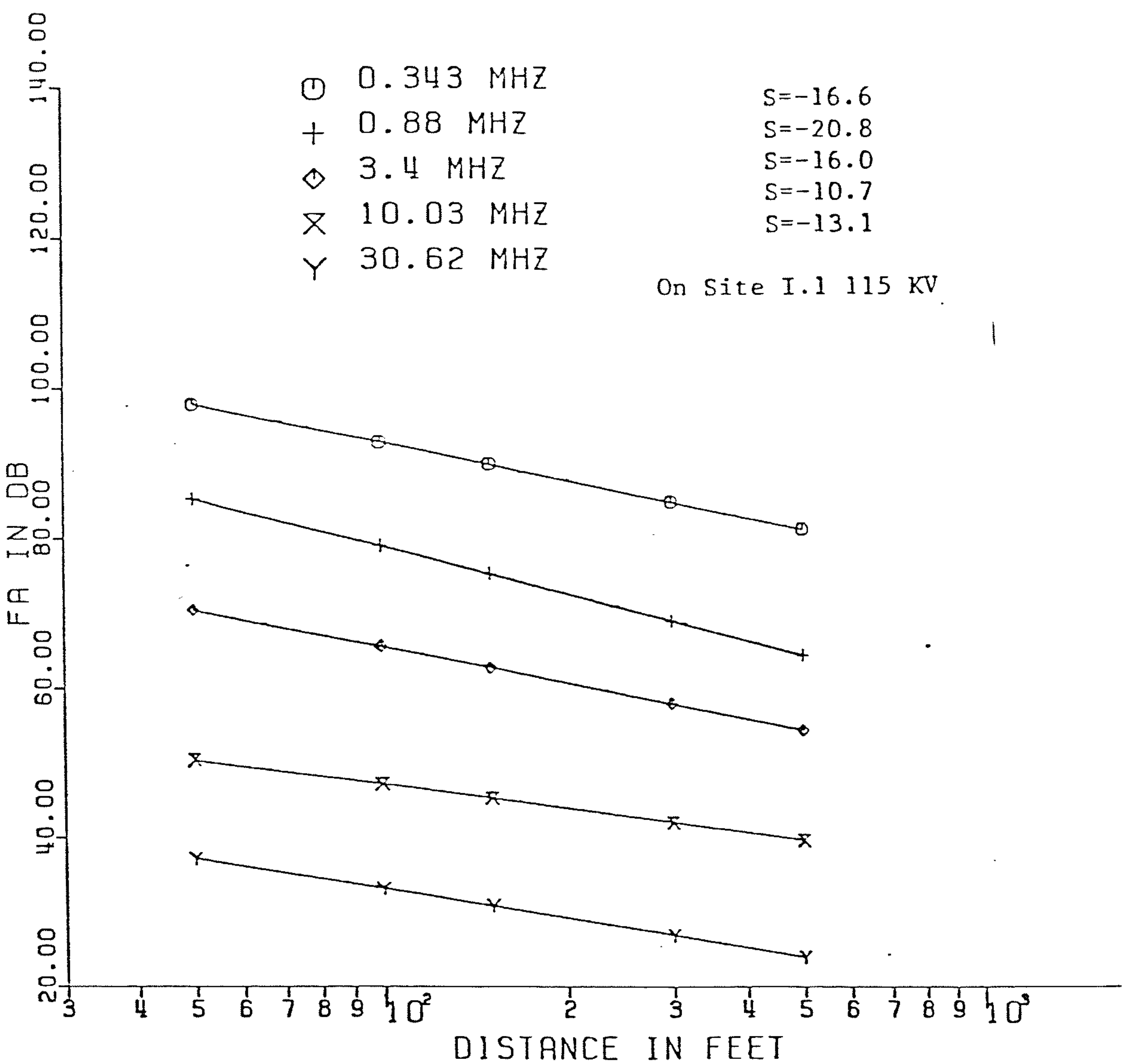

Figure (6g)

Variation of noise with distance having the frequency as a parameter.

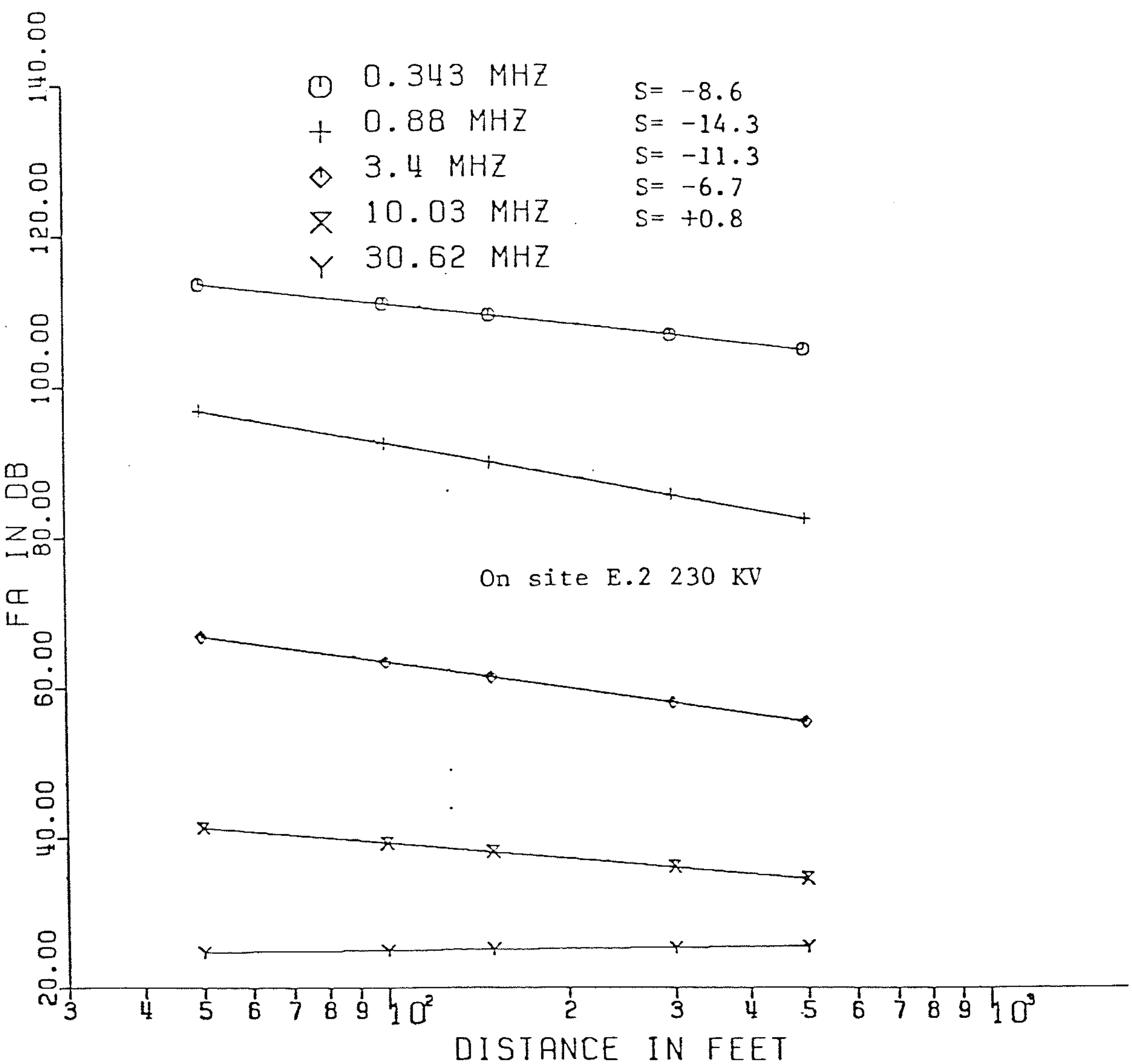

Figure (6h)

Variation of noise with distance
having the frequency as a parameter.

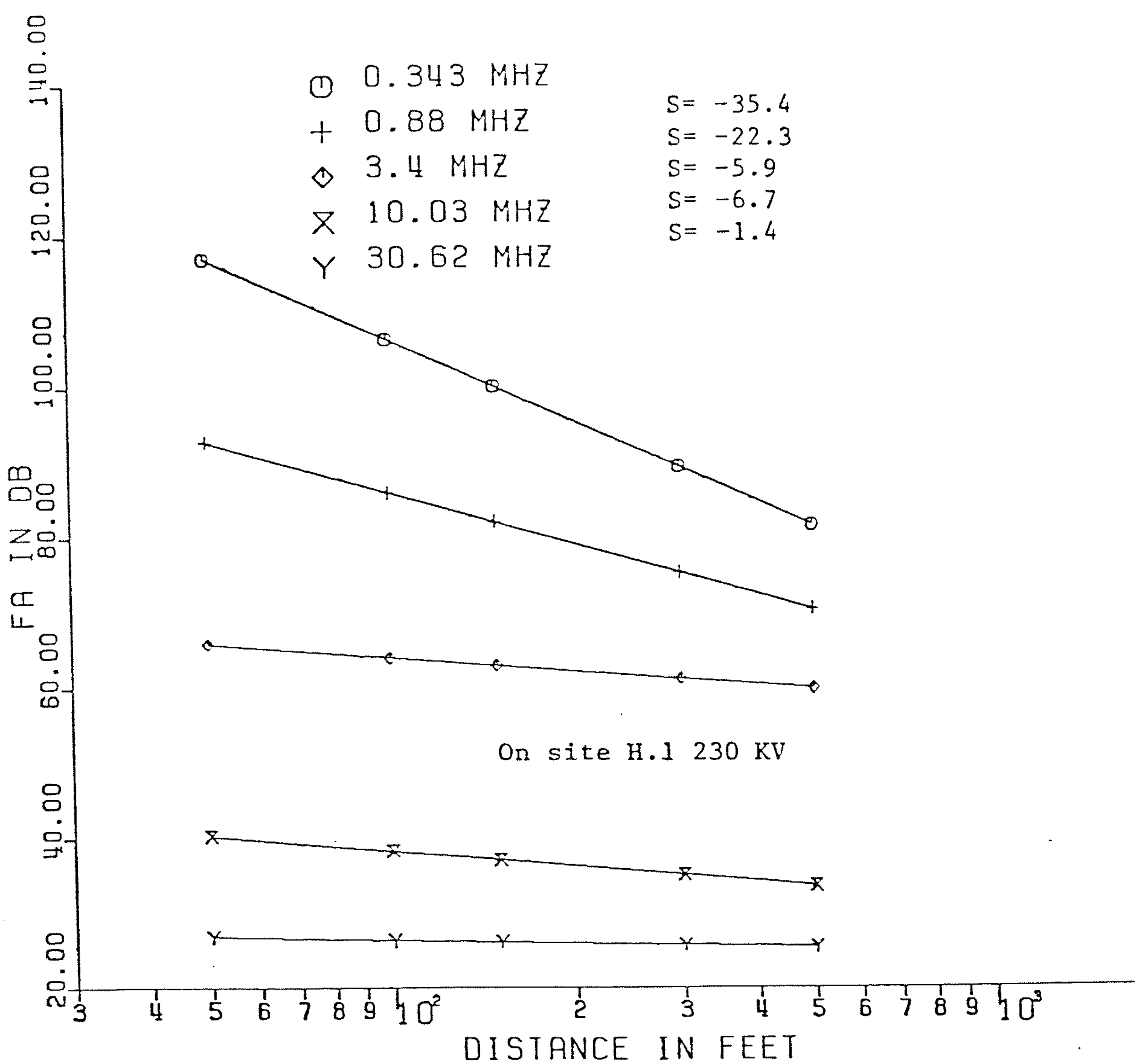

Figure (6i)

Variation of noise with distance having the frequency as a parameter.

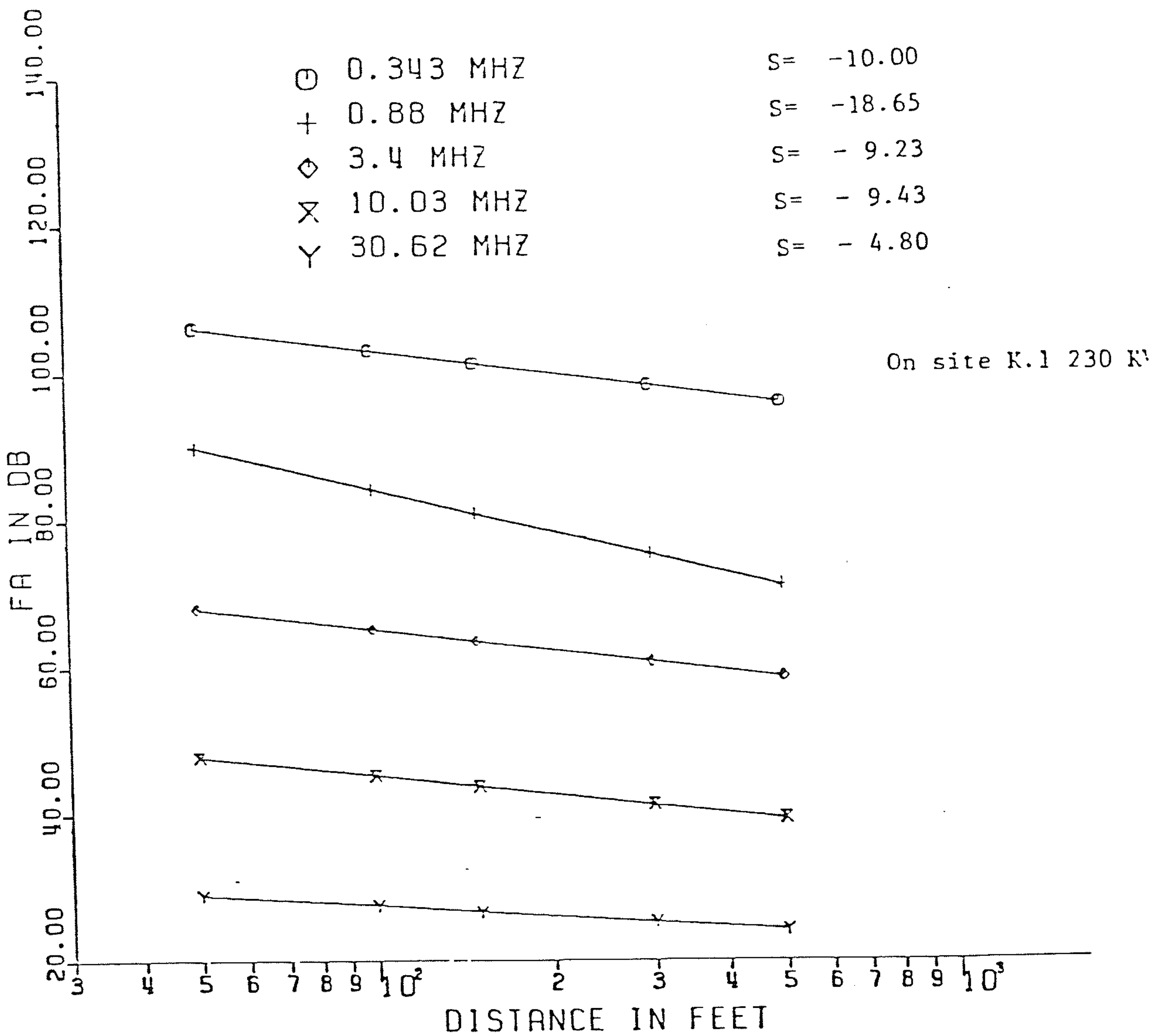

Figure (6j)

Variation of noise with distance having the frequency as a parameter.

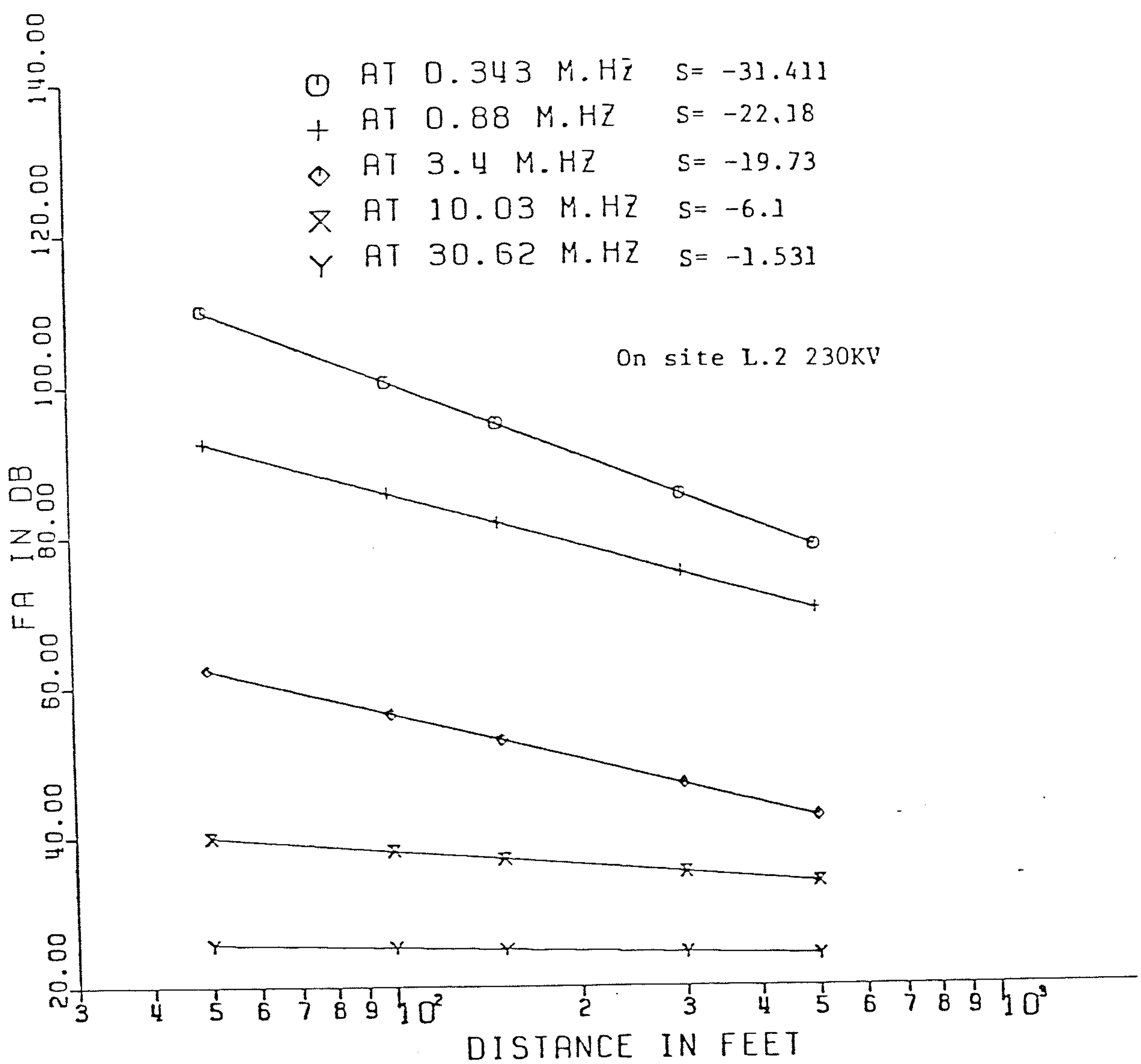

Figure (6k)

Variation of noise with distance having the frequency as a parameter.

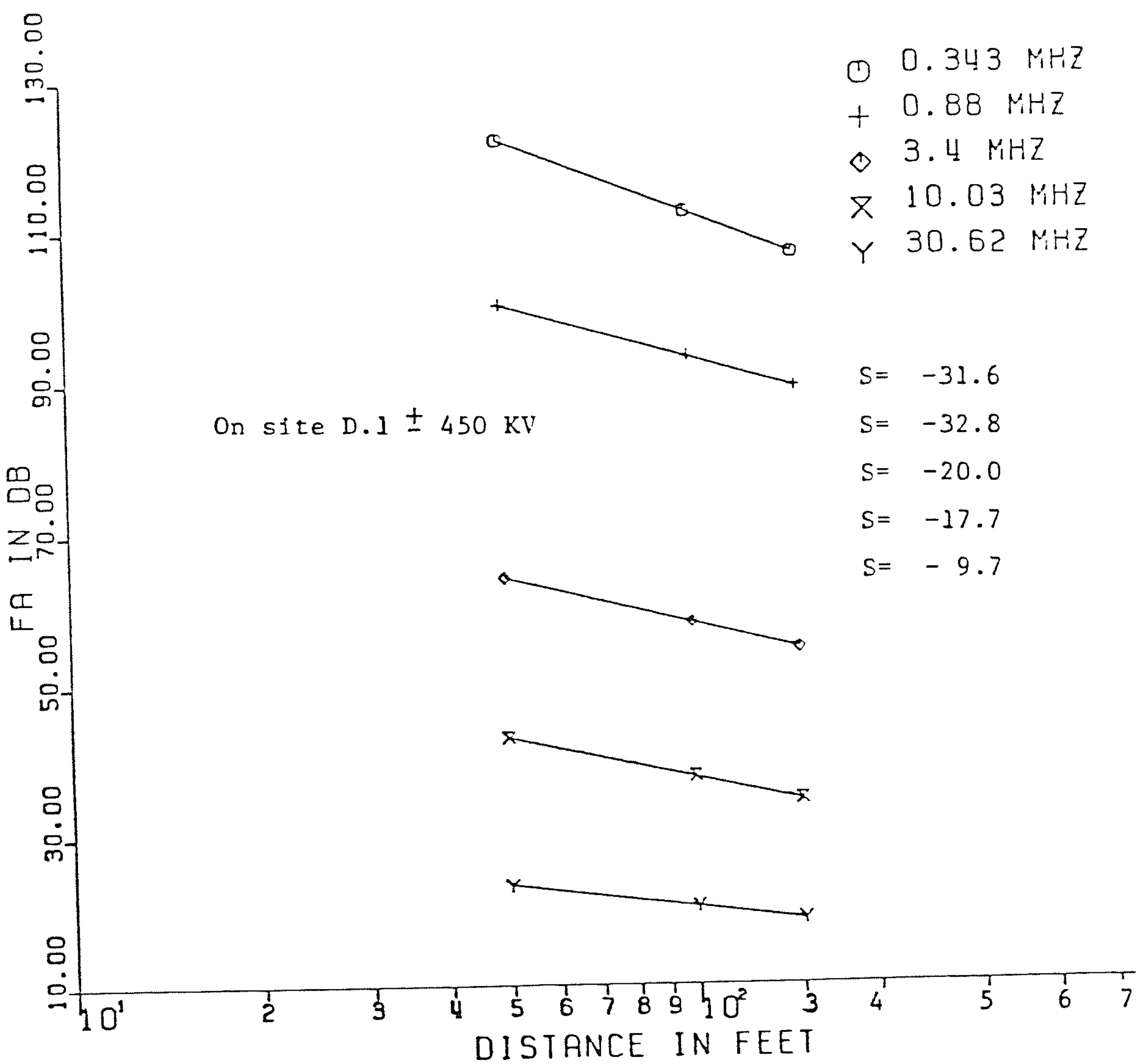

Figure (61)

Variation of noise with distance having the frequency as a parameter.

Figure	Site	Voltage in KV	Slope (dB/decade)
6a	N.1	12	-15.20
6b	M.2	66	-17.40
6c	M.1	66	-27.50
6d	A.1	115	-10.20
6e	B.3	115	-25.00
6f	G.1	115	-20.30
6g	I.1	115	-16.60
6h	E.2	230	- 8.60
6i	H.1	230	-35.40
6j	K.1	230	-10.04
6k	L.2	230	-31.41
6l	D.1	±450	-31.60

Table (4)

Slopes of F_a models with distance obtained from figures (6a-l) at 0.343 MHz.

increasing distance. In order to further illustrate this observation, table (4) shows the F_a decrease with distance at the frequency of 0.343 MHz.

The correlation coefficient, for the results presented in table (4), ranged from 0.7 to 0.99. This shows a good fit of the F_a values with respect to distance. In table (5), the correlation coefficients for the results obtained at 0.88, 3.4, 10.03 and 30.62 MHz are presented. The values of the correlation coefficient were, on the majority, greater than 0.7 with the exception of those values obtained for sites E.2 and L.2 (230 KV) at a frequency of 30.62 MHz. In fact, one expects the noise levels at 30.62 MHz to be approximately a constant value due to atmospheric noise [18], which is dominant at that frequency. In other words, the noise received at 30.62 MHz is not that of the power line but it is atmospheric. It is seen from figures (6a-1) that even out to the maximum measurement distance, the F_a levels do not decrease dramatically. This result shows that even at large distances from the power line, one can expect a significant amount of power line noise, particularly at frequencies lower than 10.03 MHz. As an example, it is seen from figure (6a) that at 0.343 MHz and at a distance of 1000 feet, one expects an F_a value of 80 dB. At 50 feet and at the same frequency, one expects an F_a value of 93 dB which is only 13 dB higher that the F_a value obtained at 1000 feet.

Table (5)
The correlation coefficients
for results presented in figures (6a-1).

Frequency	Site	Voltage	Correlation Coefficient
0.88 MHz	N.1	12 KV	0.84
	M.2	66 KV	0.88
	M.1	66 KV	0.97
	A.1	115 KV	0.90
	B.3	115 KV	0.98
	G.1	115 KV	0.68
	I.1	115 KV	0.86
	E.2	230 KV	0.87
	H.1	230 KV	0.94
	K.1	230 KV	0.92
	L.2	230 KV	0.91
	D.1	±450 KV	0.99
3.40 MHz	N.1	12 KV	0.84
	M.2	66 KV	0.81
	M.1	66 KV	0.85
	A.1	115 KV	0.86
	B.3	115 KV	0.96
	G.1	115 KV	0.59
	I.1	115 KV	0.96
	E.2	230 KV	0.59
	H.1	230 KV	0.89
	K.1	230 KV	0.89
	L.2	230 KV	0.84
	D.1	±450 KV	0.97

Table (5) (continued)

Frequency	Site	Voltage	Correlation Coefficient
10.03 MHz	N.1	12 KV	0.78
	M.2	66 KV	0.99
	M.1	66 KV	0.62
	A.1	115 KV	0.77
	B.3	115 KV	0.88
	G.1	115 KV	0.66
	I.1	115 KV	0.91
	E.2	230 KV	0.51
	H.1	230 KV	0.76
	K.1	230 KV	0.78
	L.2	230 KV	0.61
	D.1	±450 KV	0.98
30.62 MHz	N.1	12 KV	0.83
	M.2	66 KV	0.95
	M.1	66 KV	0.98
	A.1	115 KV	0.72
	B.3	115 KV	0.87
	G.1	115 KV	0.86
	I.1	115 KV	0.99
	E.2	230 KV	0.23
	H.1	230 KV	0.73
	K.1	230 KV	0.68
	L.2	230 KV	0.46
	D.1	±450 KV	0.98

The models obtained for all power lines tested, those presented in figures (6a-1), can be used to predict the amount of signal degradation due to noise from any of these lines at different distances out to 500 feet. The relationship between F_a and the logarithm of distance for each individual line can be obtained from the figures with the knowledge of its slope and its intersection with the F_a axis. An example of such a relationship, as can be obtained from figure (6a) is as follows:

Slope (at 0.343 MHz)= -15.23 dB/distance decade,

Intersect with F_a axis (from program)= 120.0 dB,

Confidence interval= 7.0 dB.

Thus:

$$F_a = 120 - 15.23 \log d \pm 3.5$$

An attempt may be made to interpret the results in terms of radiations from known simple source models, for example, cylindrical source or a set of incoherent point sources. In case of point source radiator the model slope is theoretically 40 dB/decade at near field and 20 dB/decade at far field.

W. E. Pakala [21] suggested that a power line can be represented by an infinite linear radiator. R. F. Harrington [22] obtained the Electromagnetic field equations for such a radiator and he showed that at far field the amplitude of the waves decreases as $r^{-\frac{1}{2}}$ (which corresponds to 10 dB/distance decade). Comparing the above figures with those obtained in figures (6a-1), it is seen that 50% of the slopes at near field were close to a value of 20$\pm$7 dB/decade and 75% to 10 $\pm$ 4 dB at far field. The agreement between the slopes obtained from the data and these theoritical values shows that the lines behave like an infinite linear radiator. A study, depending on the needed accuracy, may require extensive frequency as well as physical profile measurements and is recommended for future research.

4.3.3 F_a versus Voltage relationship

Since loading conditions on a power line fluctuate continuously, depending on the consumption at any given time, the line voltage will accordingly deviate from its rated value. This deviation in line voltage produces a change in the noise levels emitted by the power line. To illustrate this fact, the line with the greatest range of voltage deviation from its rated value was chosen. This line is at site H.1 (230 KV). A computer program was written to apply linear regression to the F_a values obtained for all visits made to this line, with respect to the line voltage. Figure (7) shows the resulting plots for frequencies of 0.343, 3.4 and 30.62 MHz at the first location. The figure indicates a slight increase in F_a level with increase in line voltage. This increase is presented in table (6). The correlation coefficient ranged from 0.8 to 0.97. This shows that the linear regression gave a good fit to the F_a values, presented in figure (7).

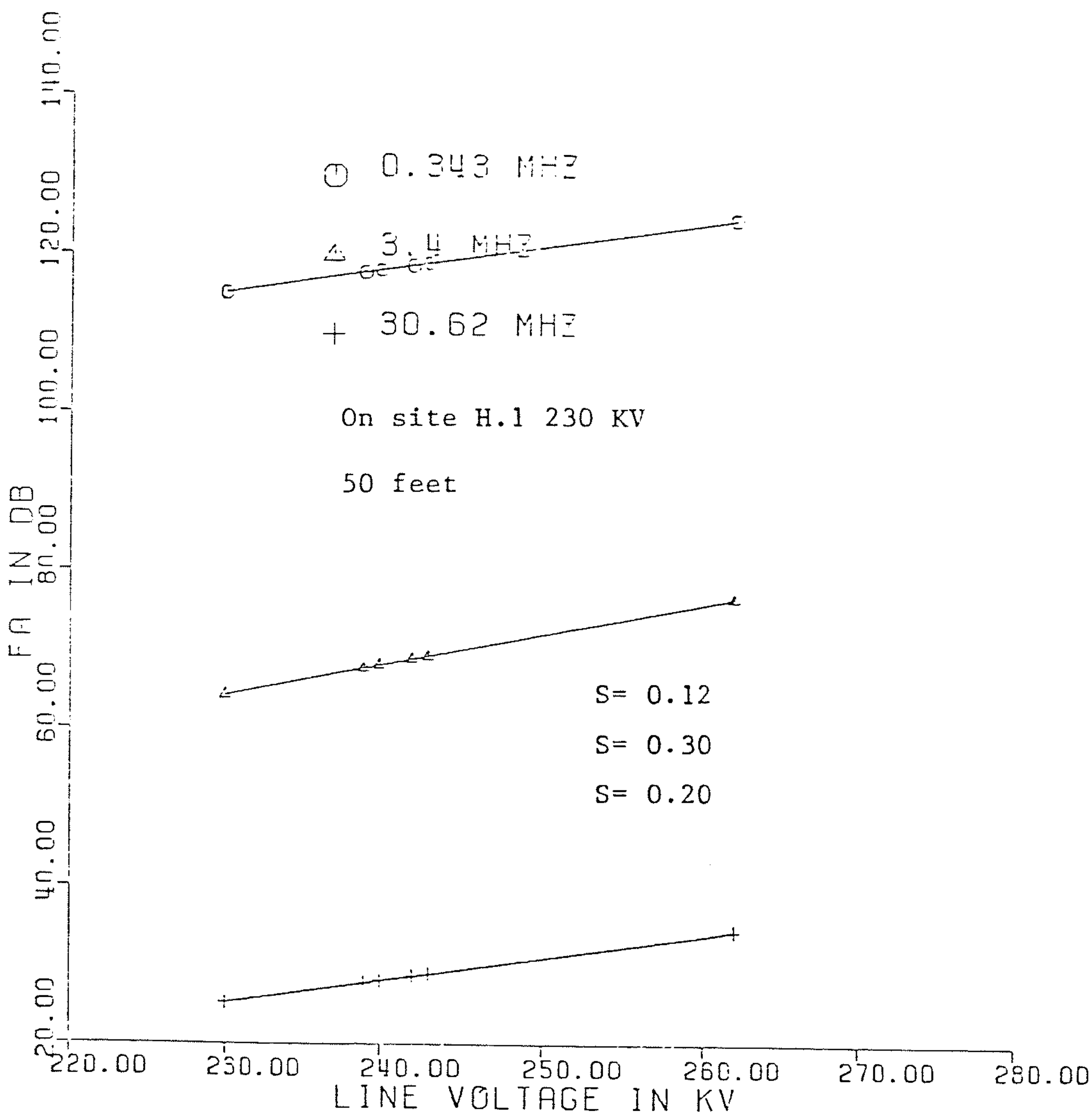

Figure (7)

The noise level variation with
small variations in line voltage .

Frequency	Slope dB/KV
0.343 MHz	0.12
3.4 MHz	0.3
30.62 MHz	0.2

Table (6)

Slopes of F_a versus V relationship obtained from site H.1 (230 KV).

The relationship between the noise levels of each power line class with respect to line voltage was also obtained. In order to obtain this relationship, F_a values that were measured from lines that had the same line voltage, were averaged in order to obtain an F_a value that represented that particular voltage class. The averaging was done for F_a values obtained at the same frequency and the same location. This procedure was repeated for all the AC voltage classes, resulting in an array of F_a values, each of which represented an average value of F_a obtained at each class. A computer program was prepared to apply linear regression to the F_a array against the line voltage of the these lines. The program obtains the F_a versus log V relationship at a location 50 feet from the lines and at all test frequencies. The program was adjusted so that only three models of the F_a versus log V relationship at frequencies of 0.343 ,3.4 and 30.62 MHz are plotted. The results of this program are given in figure (8) and it is seen that the F_a levels increase with an increase in line voltage. This increase is presented in table (7). From table (6) and table (7), it is seen that the slopes of both relationships obtained in figures (7) and (8), agree very well at the frequencies of 0.343 and 3.4 MHz. A desirable alternative to obtain the F_a variation with respect to line voltage is to apply the linear regression to all the values of F_a obtained from all visits from a given line. It is seen, from figure (8), that one expects a noise level of 82 dB from the 12 KV class at 0.343 MHz. The 230 KV class produces a noise level of 114 dB, which is 32 dB

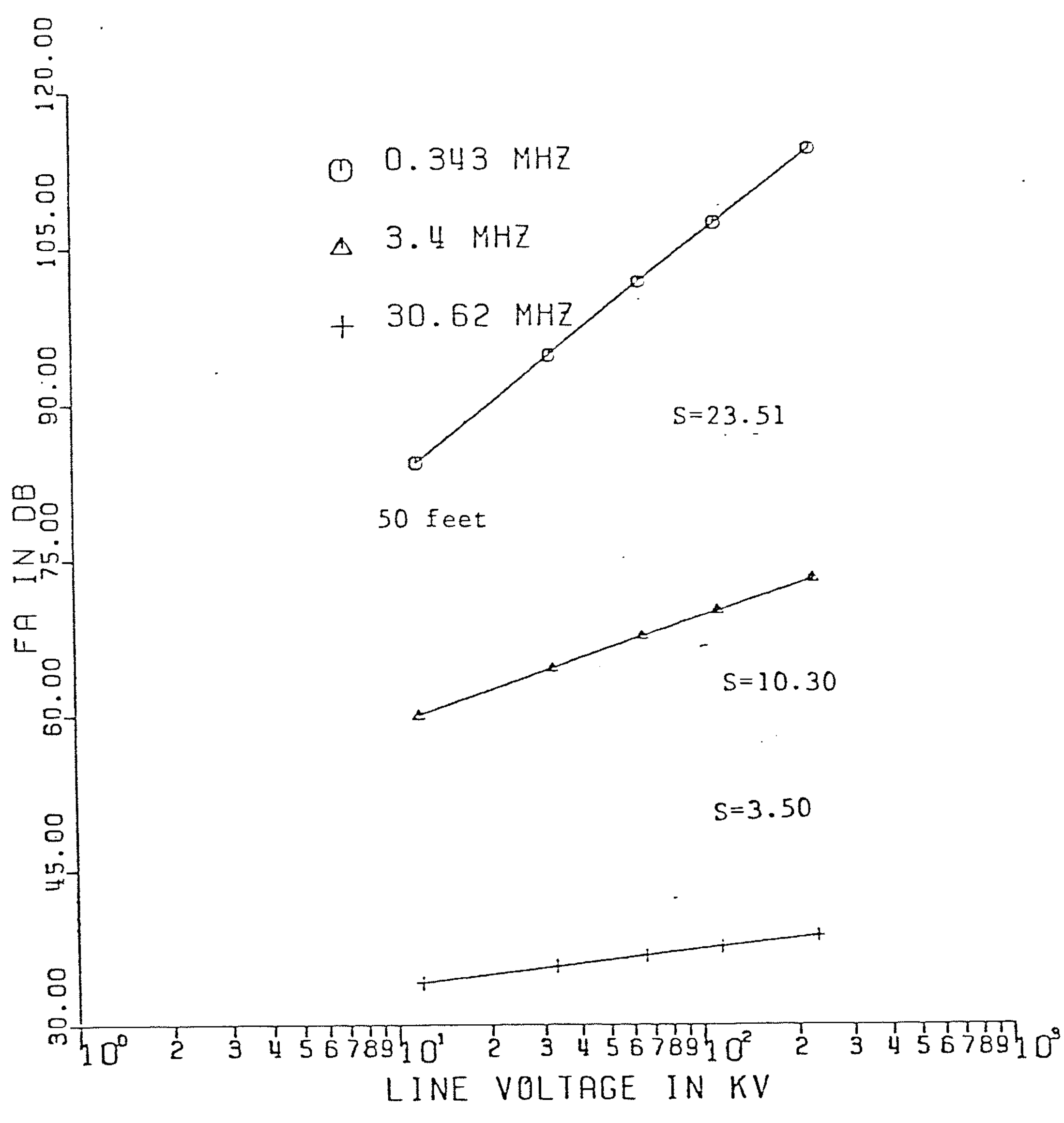

Figure (8)

The noise levels variation with the variation in line voltage.

Frequency	Slope dB/decade	Slope dB/KV
0.343 MHz	23.51	0.1
3.4 MHz	10.30	0.23
30.62 MHz	3.50	0.03

Table (7)

Slopes of F_a versus log V relationship for the five AC voltage classes.

higher than the 12 KV class, assuming that the noise is received at the same frequency.

4.4 APPLICATION OF LINEAR REGRESSION TO V_d

For each site the V_d values obtained at the 50 feet location from all visits were averaged at each of the nine test frequencies in order to characterize the noise type. Linear regression was applied using a computer program to obtain the V_d variation with respect to frequency. The procedure was repeated for the other four locations at each site with lateral profiles.

Plots of the voltage deviation versus frequency are given in figure (9a-c). The correlation coefficients for V_d versus log f graphs were very low (with a range from 0.1 to 0.8 with most factors falling below 0.3). The low correlation factors indicate that V_d is uncorrelated to frequency, through the linear regression. A higher order modeling technique would probably provide a better fit to the V_d versus log f relationship. An example for V_d versus log f with a correlation coefficient of 0.7, at 50 feet is shown in figure (9a). From the figure, it is seen that V_d values have an average which ranges from 2 to 3 dB. In figure (9c), the voltage deviation relation with frequency on the DC line shows a maximum average value of 4.3 dB which is higher than that value obtained for all AC line classes.

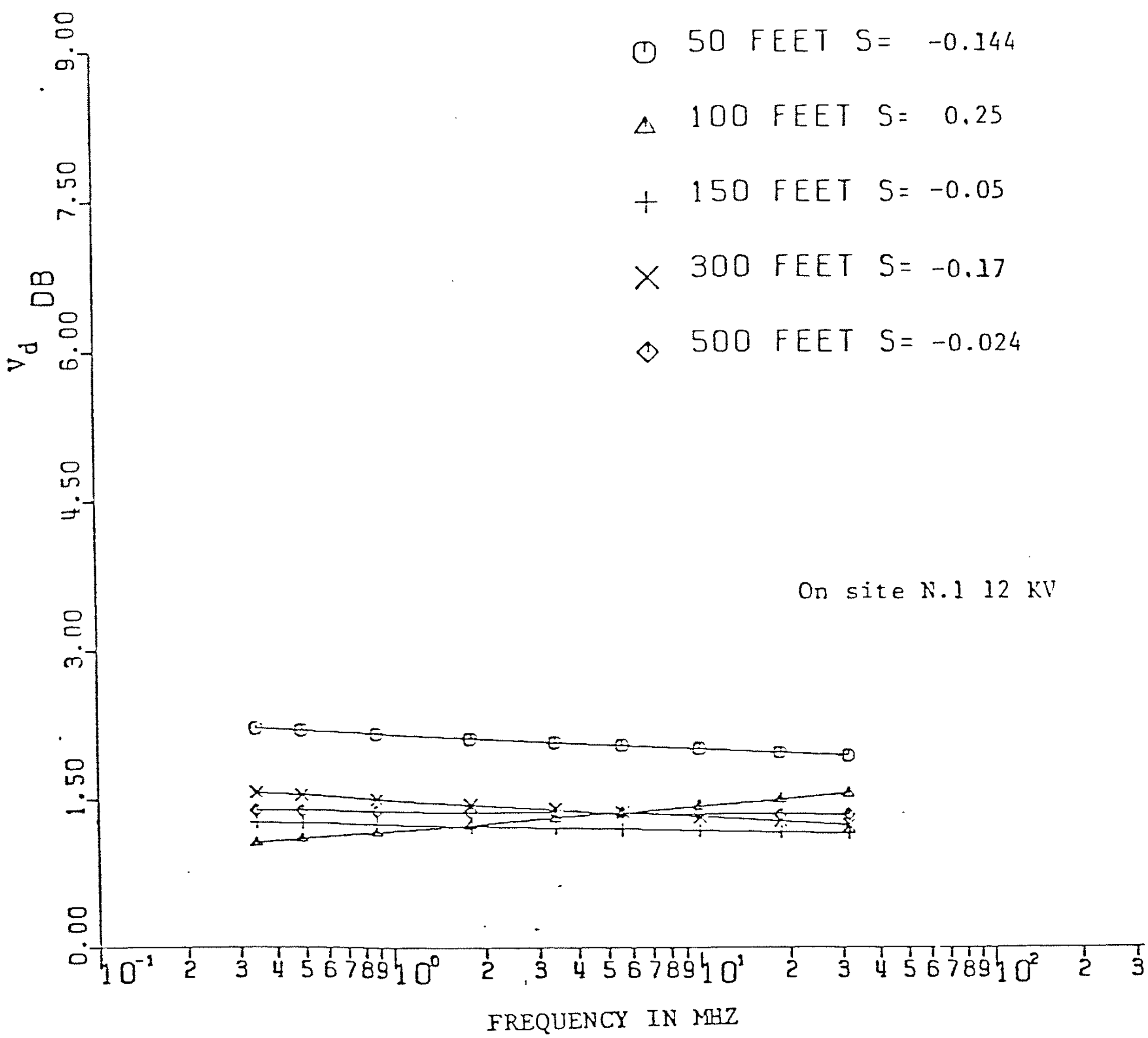

Figure (9a)

The voltage deviation variation with frequency having the distance as a parameter.

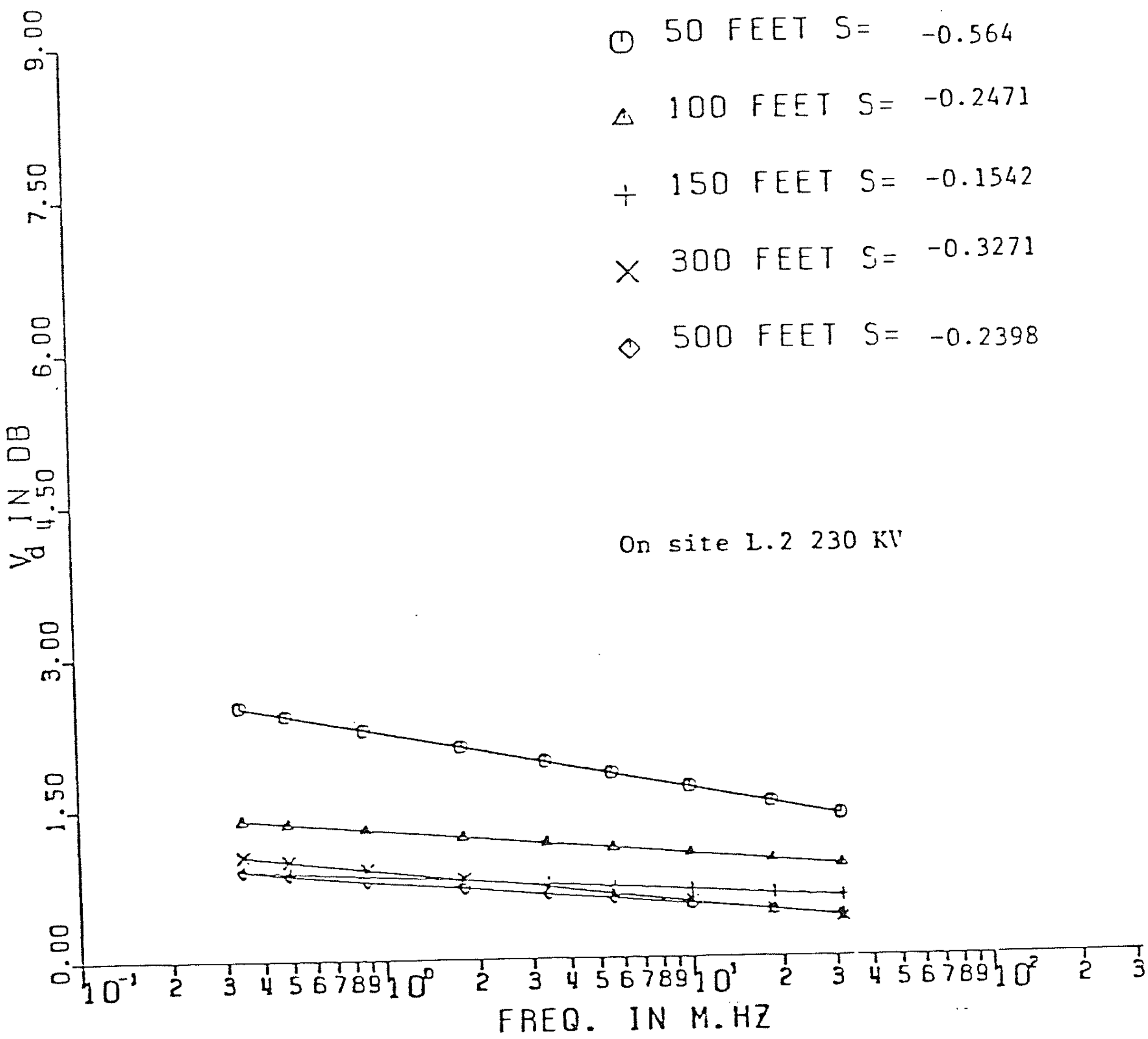

Figure (9.b)

The voltage deviation variation with frequency having the distance as a parameter.

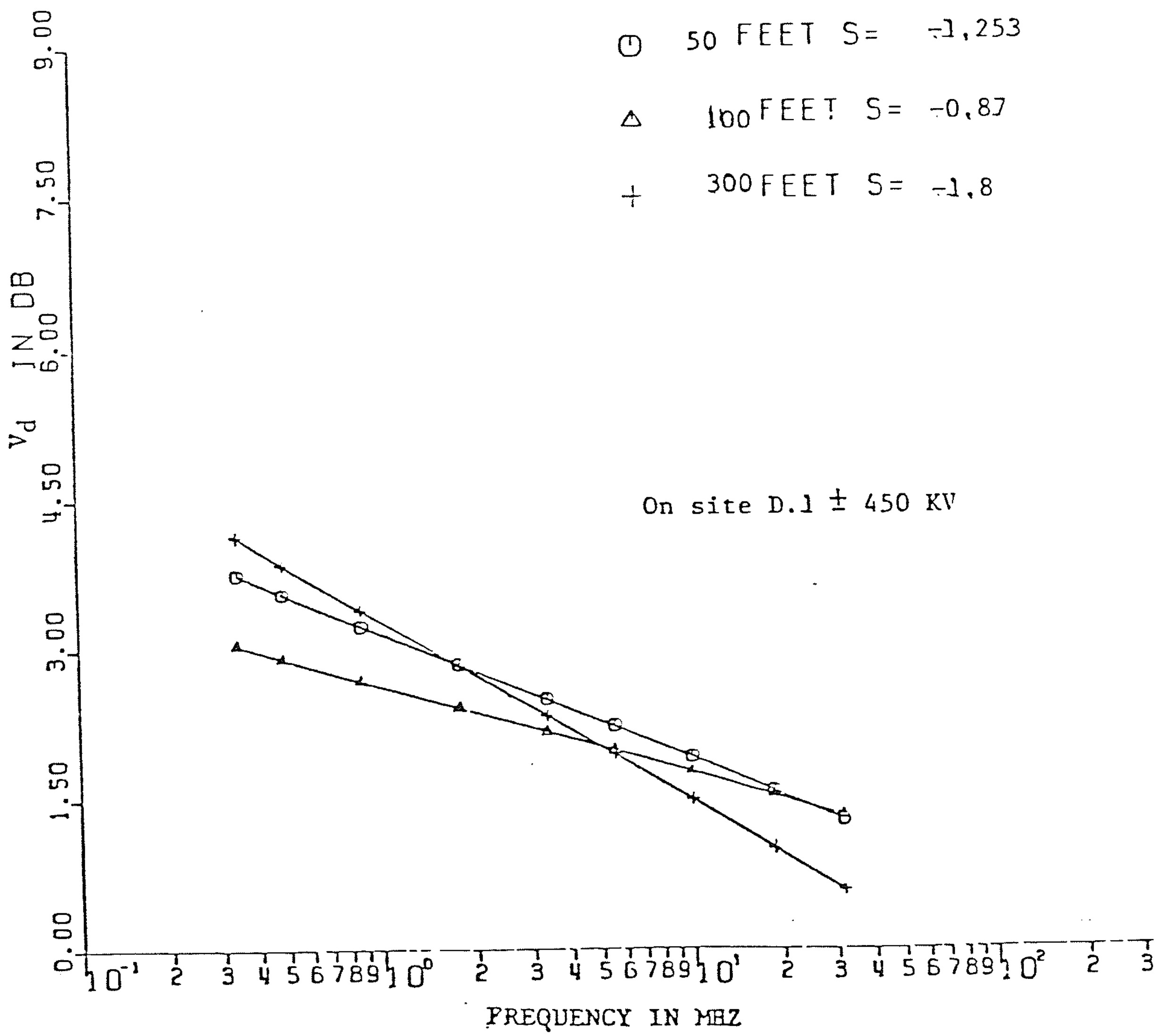

Figure (9c)

The voltage deviation variation with frequency having the distance as a parameter.

4.5 EFFECTS OF WEATHER CONDITIONS ON F_a LEVELS

Although the effects of changing weather conditions on F_a levels were a desired objective of the project, insufficient data to produce a comprehensive result were collected. A sample of the relationship between F_a levels and changing weather conditions was obtained from site B.3 (115 KV). A computer program was used to obtain the result presented in figure (10). The figure shows the effects of rain, fair weather and light snow on F_a values obtained from visits 2, 5 and 9, respectively. In the figure, it is seen that at a frequency of 3.4 MHz, F_a was 90 dB when it was raining, 82 dB when light snow was falling and 71 dB when the weather was fair.

4.6 EFFECTS OF LINE LOADING ON NOISE LEVELS.

Measurements on one unloaded line (M.1 66 KV), depicted in figure (5c), shows that noise levels are 23 dB higher than those obtained from the same portion of the line which was loaded (M.2 66 KV), shown in figure (5b). The noise levels of the unloaded line are even higher than the noise received from the 115 KV lines. These levels are high enough to severely contaminate an AM broadcast signal that a receiver would detect if it were located at fifty feet from the line. The field strength voltage of the noise at 1 MHz at that location is 57.5 dBμV/m (as will be shown in section

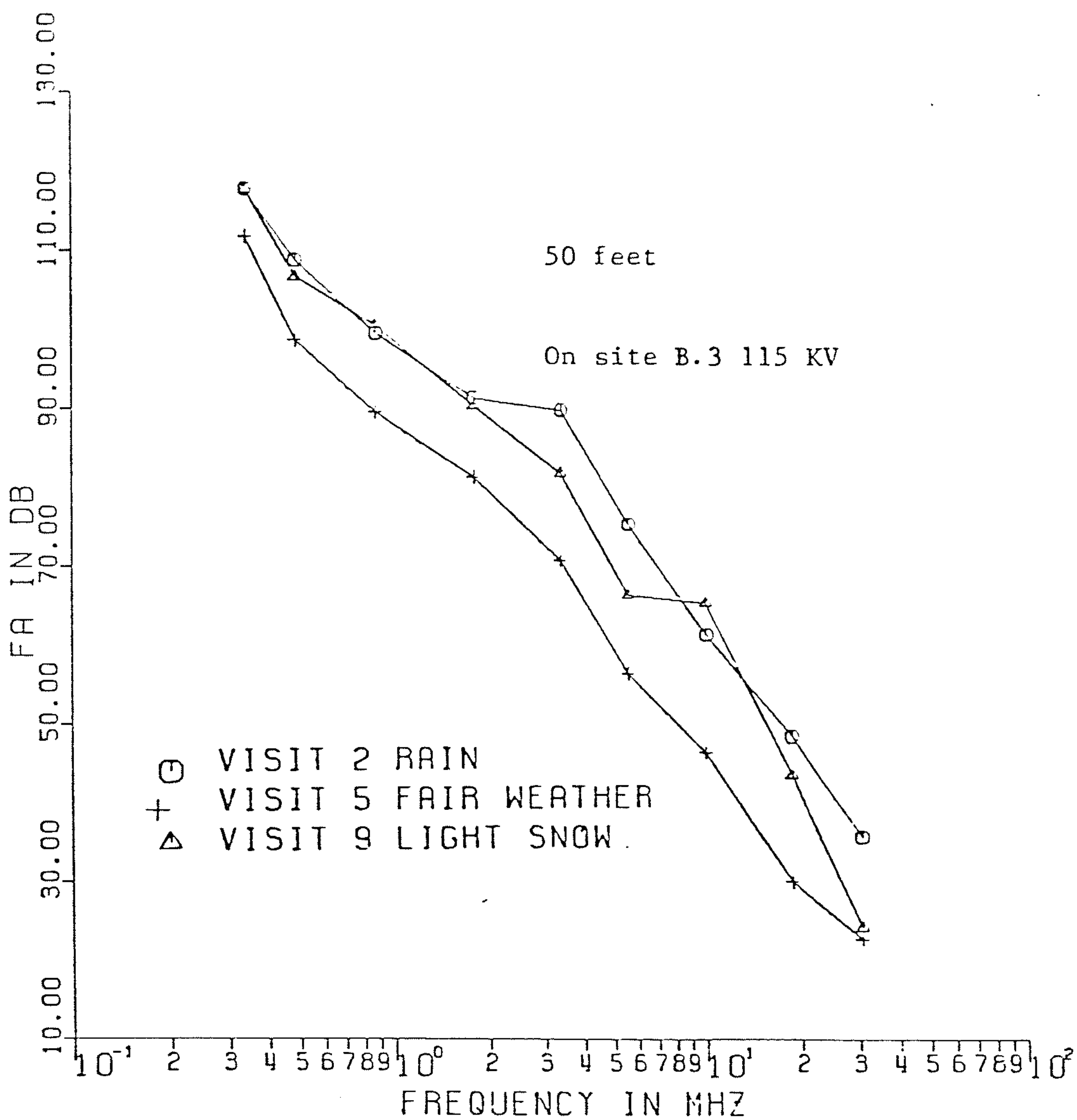

Figure (10)

The effects of weather conditions
on the received noise spectra.

4.8). Keeping in mind that radio signal strength is higher than the lowest protected strength contour (54 dB μ V/m) [1], one can predict that a severely noise contaminated radio signal at that frequency would be detected by the receiver.

4.7 COMPUTED NOISE PREDICTION MODELS.

In section 4.3.1, a model of F_a in terms of frequency for each power line was obtained. The F_a models obtained for lines that had the same voltage, were averaged in order to obtain an over-all model of F_a in terms of frequency for each voltage class of power line.

The 12 and 33 KV voltage classes were represented by site N.1 and site C.3 respectively. This was due to the fact that these were the only sites in the region surveyed with these line voltages that were monitored by Manitoba Hydro. Site M.2 (66 KV) also represented its voltage class, since site M.1 (66 KV) was an unloaded line, which produced much higher noise levels than site M.2. The 115 KV voltage class model was obtained by averaging F_a versus log f models obtained for sites A.1, B.3, I.1 and G.1, while the 230 KV voltage class model was obtained from sites K.1, L.2, H.1 and E.2.

The set of models obtained for the five AC classes of power lines, in addition to the model obtained for the DC line, are given in figures (12a-e). The linear relationships computed for these classes are:

4.7.1 Models of F_a with frequency.

12 KVAC class model

$$F_a = 70.0 - 32 \log f \pm 7.25$$

33 KVAC class model

$$F_a = 69.4 - 28 \log f \pm 7.65$$

66 KVAC class model

$$F_a = 93.0 - 35.3 \log f \pm 4.0$$

115 KVAC class model

$$F_a = 88.3 - 35.5 \log f \pm 5.0$$

230 KVAC class model

$$F_a = 90.9 - 44.3 \log f \pm 6.4$$

450 KVDC class model

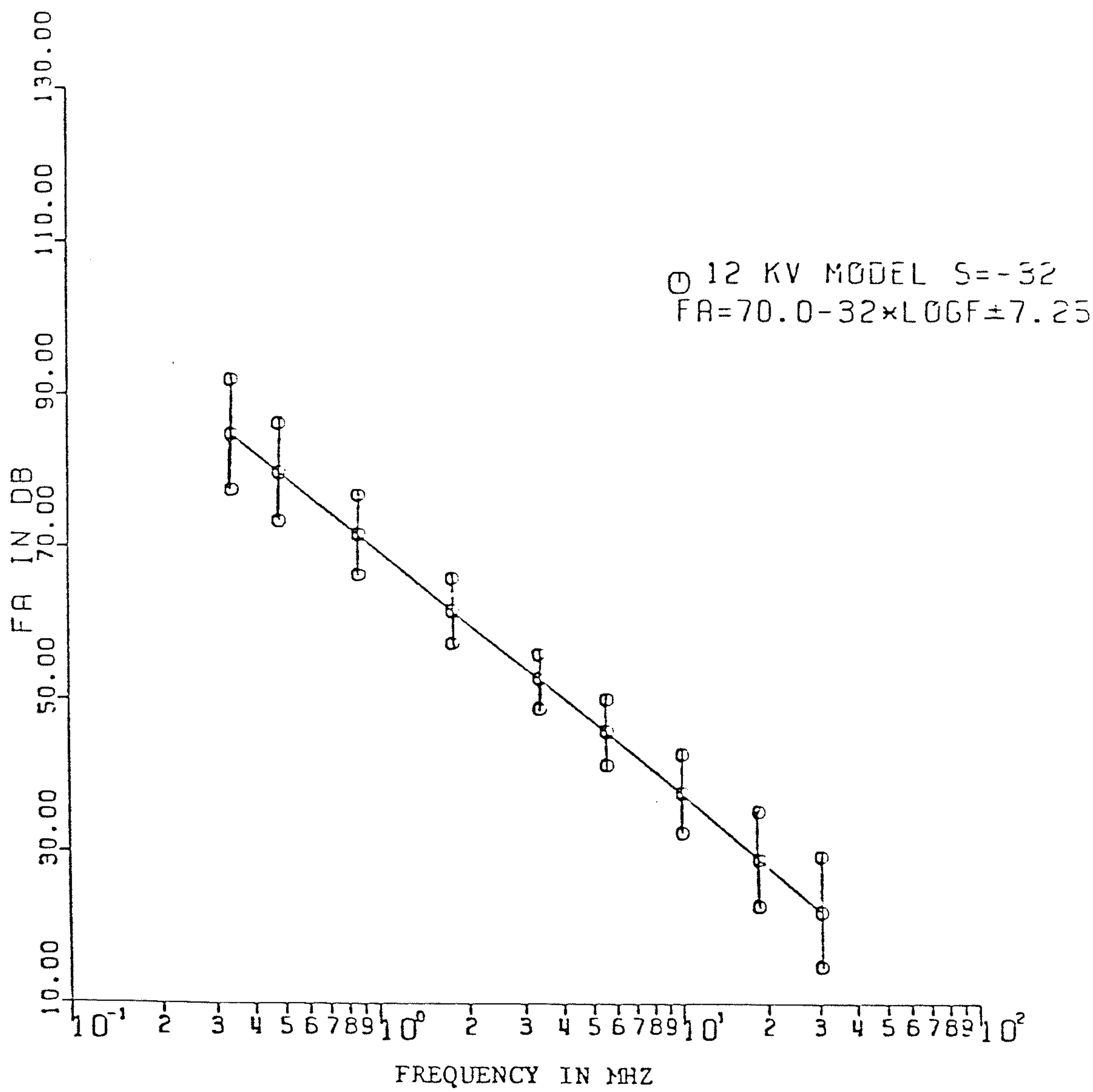

Figure (11a)

F_a versus frequency model for

the 12 KV class.

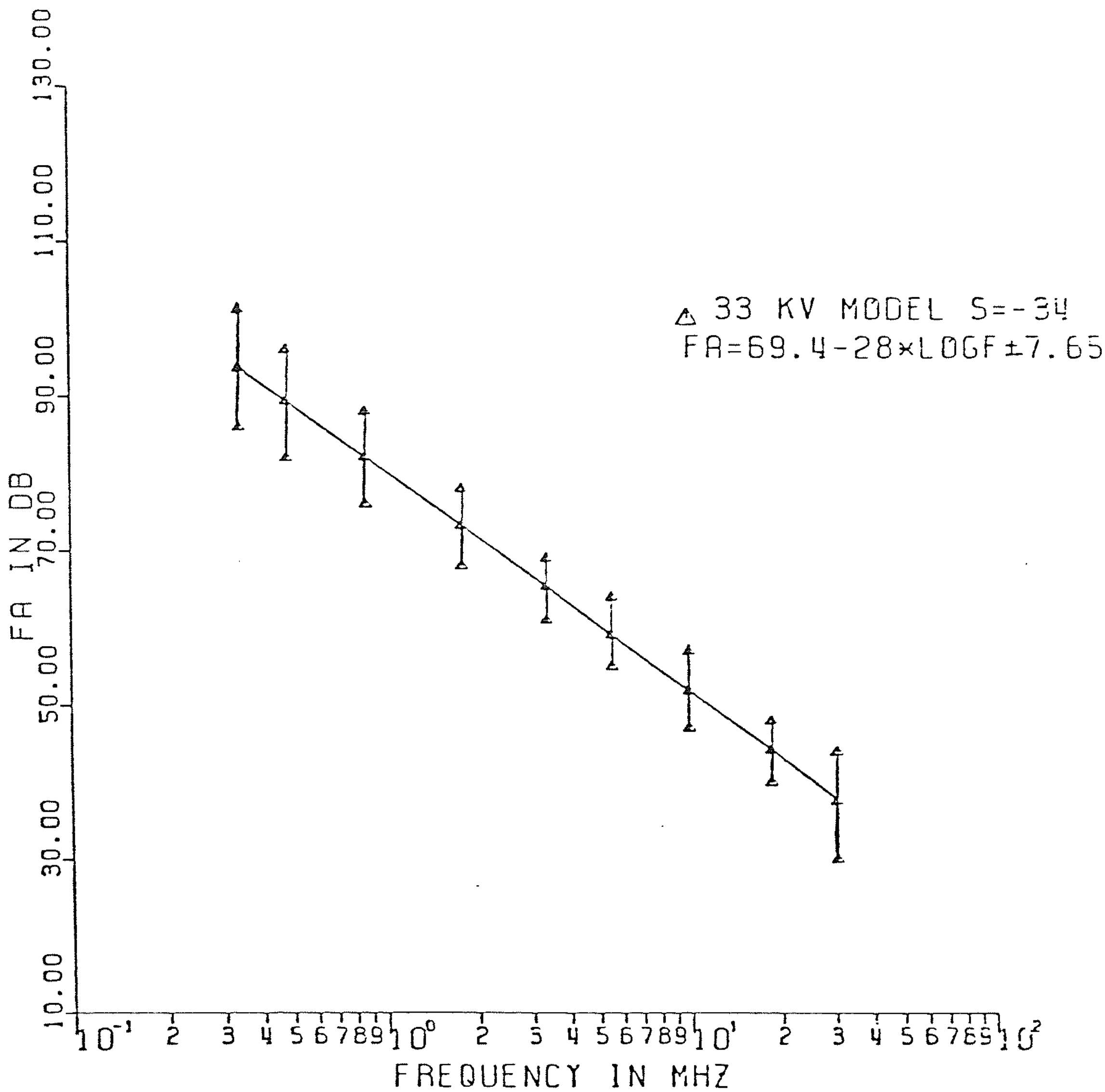

Figure (11b)

F_a versus frequency model

for the 33 KV class.

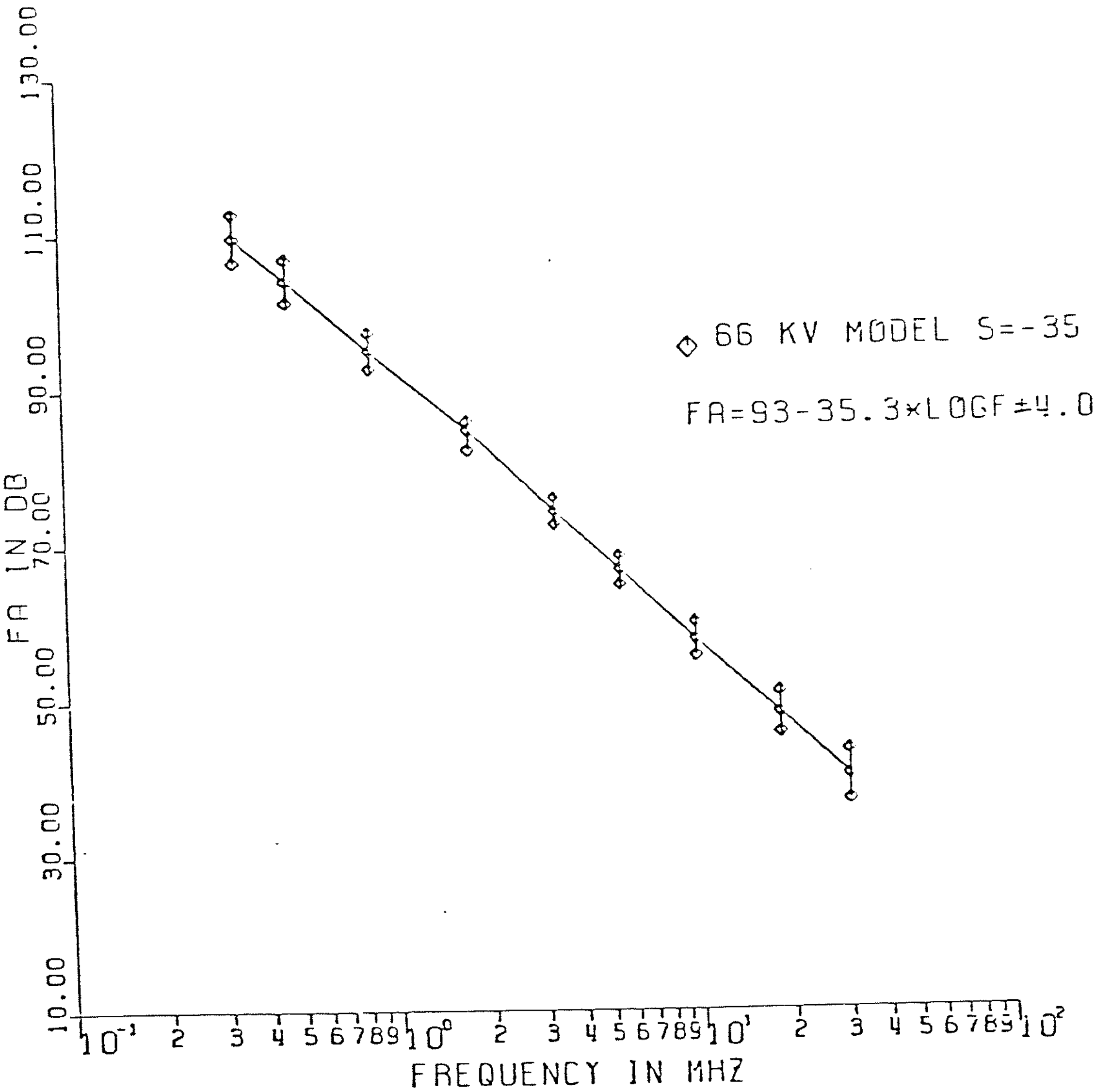

Figure (11c)

F_a versus frequency model
for the 66 KV class.

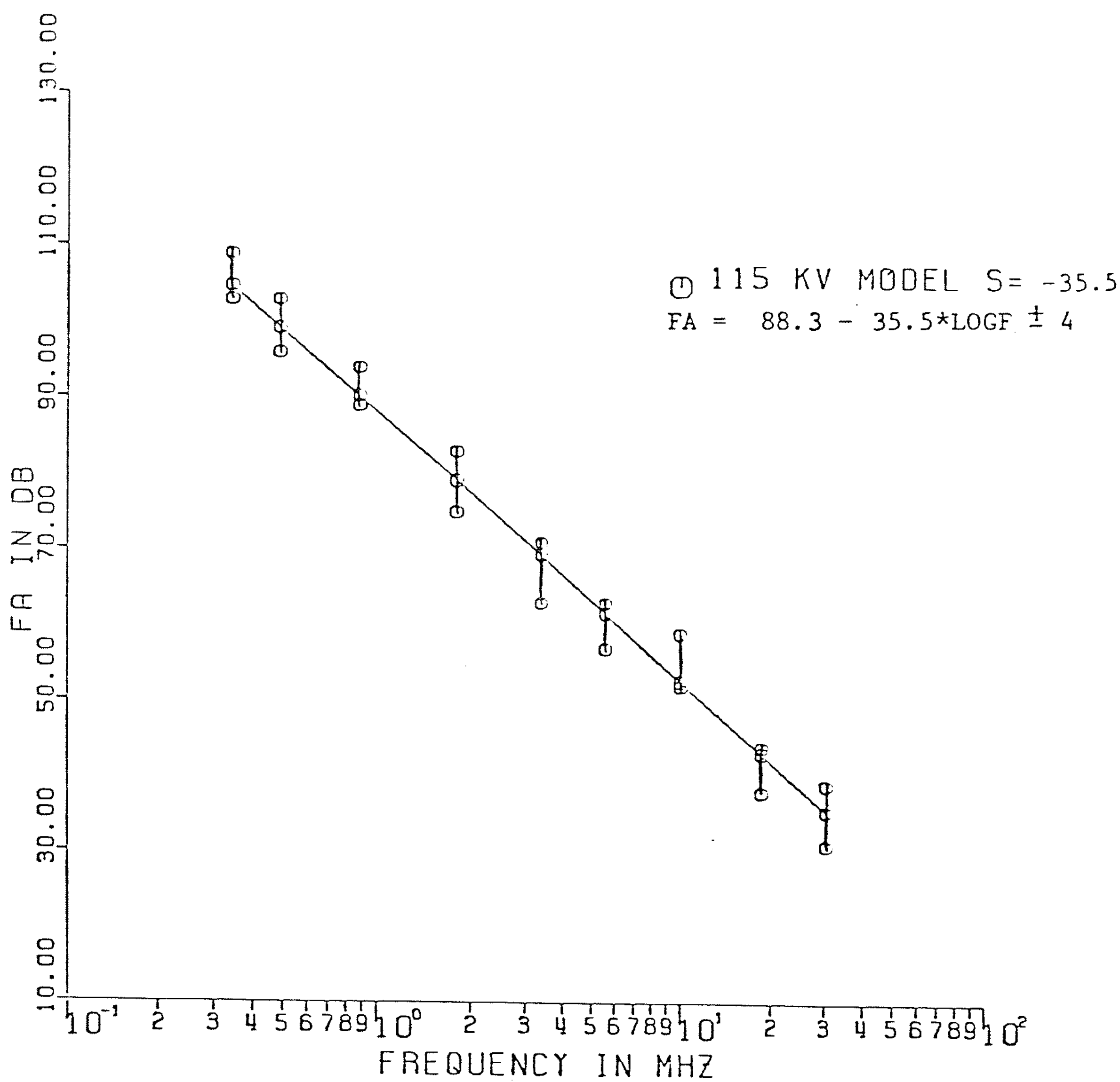

Figure (11d)

F_a versus frequency model

for the 115 KV class.

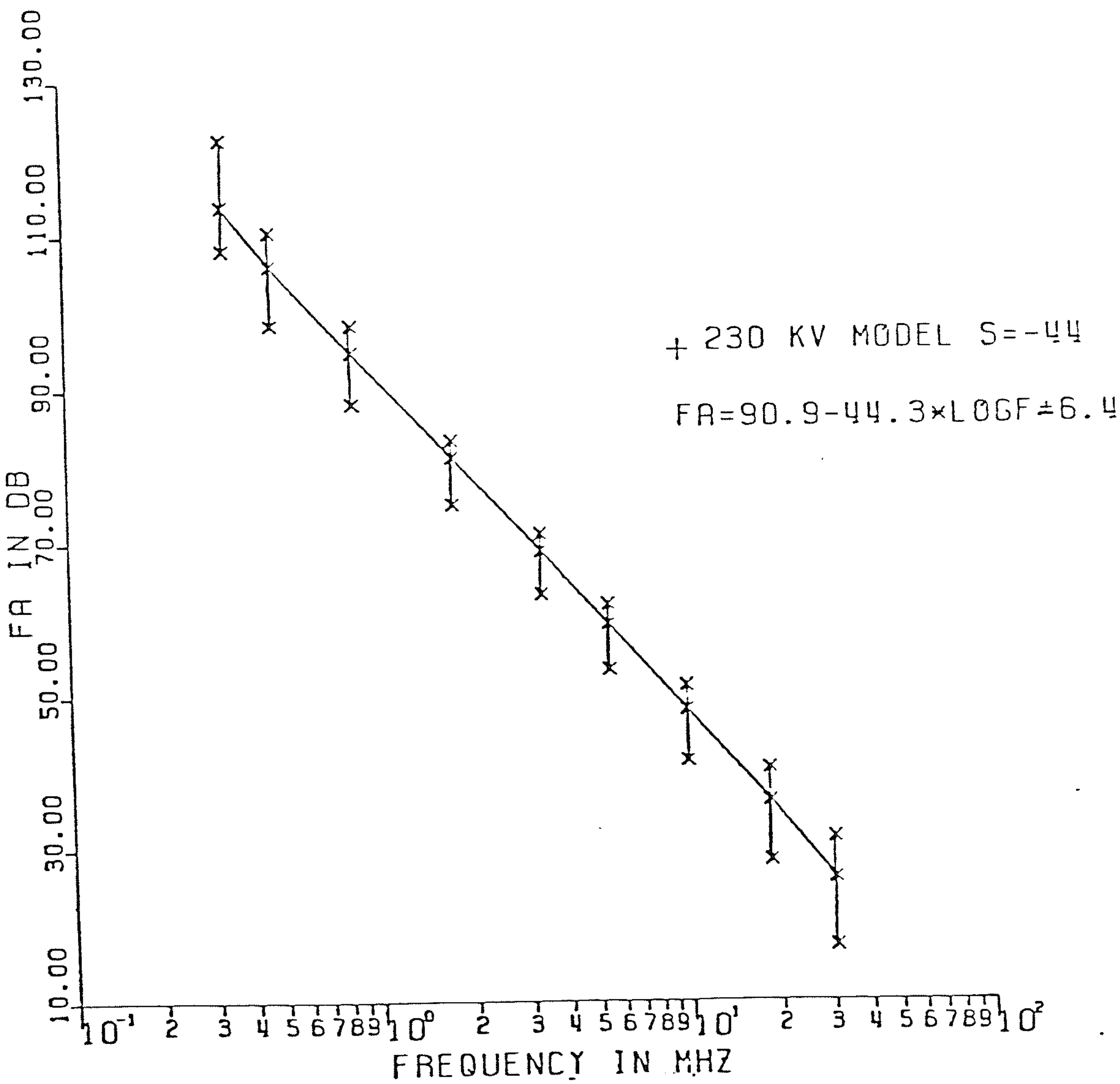

Figure (11e)

F_a versus frequency model

for the 230 KV class

$$F_a = 95.3 - 50.5 \log f \pm 6.0$$

From these models, the noise levels of any of the above classes of transmission lines can be predicted as a function of frequency at fifty feet from the center of the line.

4.7.2 Models of F_a with distance.

In section 4.3.2, a model of F_a versus log d relationship was obtained for those power lines where a profile measurement was performed. As seen from table (4), different lines of the same line voltage class produced noise models with significantly different slopes. For example, the power lines representing the 115 KV class produced noise models of slopes with a range from -10 to -25 dB/distance decade. The high difference among the slopes did not allow us to obtain an over-all model of F_a versus distance relationship for each voltage class by the averaging method as obtained for the F_a versus log f relationship. The set of models of F_a variation with distance were obtained for each individual line with the exception of site C.2 (33 KVAC) and site L.1 (230 KV), where no profile measurements were performed. These models are:

Site N.1 (12 KVAC) model

$$F_a = 120 - 15.22 \log d \pm 5$$

Site M.2 (66 KVAC) model

$$F_a = 137.3 - 17.4 \log d \pm 10$$

Site A.1 (115 KVAC) model

$$F_a = 118.7 - 10.21 \log d \pm 8$$

Site B.3(115 KVAC) model

$$F_a = 157.1 - 25.0 \log d \pm 7$$

Site G.1 (115 KVAC) model

$$F_a = 121.4 - 20.25 \log d \pm 10$$

Site I.1 (115 KVAC) model

$$F_a = 126.0 - 16.6 \log d \pm 15$$

Site K.1 (230 KVAC) model

$$F_a = 123.3 - 10.04 \log d \pm 8$$

Site L.2 (230 KVAC) model

$$F_a = 163.4 - 31.0 \log d \pm 15$$

Site E.1 (230 KVAC) model

$$F_a = 177 - 20.25 \log d \pm 7.5$$

Site E.2 (230 KVAC) model

$$F_a = 128.3 - 8.6 \log d \pm 17$$

Site D.1 (450 KVDC) model

$$F_a = 173.6 - 31.6 \log d \pm 10$$

From the above relationships and at a frequency of 0.343 MHz, the noise levels from the power lines at each of the test sites, can be predicted as a function of distance. From figures (6a-1), one can also obtain the F_a versus log d relationship at frequencies of 0.88, 3.4, 10.03 and 30.62 MHz.

4.8 PRACTICAL APPLICATIONS OF THE MODELS

The computed models of F_a versus frequency can be employed to predict the effect that a power line of a certain class might have on the quality of radio reception in its vicinity. The degree of interference expected from the power line with broadcast band stations (0.535 to 1.605 MHz), is evaluated on a Signal-to-Noise ratio basis. The

S/N ratio is approximately obtained by taking the difference between the power line field strength noise voltage in dBμ V/m and 54 dB μV/m, which is the lowest protected strength contour of AM radio signals in North America [1]. This is only valid for those power lines which produce V_d values lower than 3 dB [14]. The field strength noise voltage of a power line can be calculated by obtaining the F_a value at the frequency at which the S/N ratio is to be predicted. Then, using equation (11) in the form:

$$E(dB\mu\ V) = F_a + 20 \log f + B\ (dBHz) - 96.8$$

where

B(dBHz) is the noise bandwidth of the NM-26T meter= 35.3,

$E(dB\mu\ V) = V_{rms}(dB\mu\ V) + AF$,

E is the noise field strength voltage.

When applying the above to the unloaded line, it was found that at fifty feet away from the line, radio reception would be severely impaired by the power line noise. The noise at 1 MHz was found to be 57.5 dB μV/m according to the above equation, indicating that the receiver would detect a severely noisy signal (S/N= -3.5).

For those lines that produce V_d values greater than 3 dB, the S/N ratio is calculated by taking the difference in dB μV/m, between the amplitude probability distribution (APD) of the power line noise at a given time and the lowest protected strength contour of radio signals. The APD of the power line noise can be predicted from the measured rms and deviation voltages within 5% error as given by Lauber [13].

Using the model of a typical low noise emission site (N.1 12 KV) will result in a noise prediction of about 30 dB (at the same frequency), which indicates that a receiver will have S/N ratio of 24, adequate for class B reception.

As a further illustration of the use of the models obtained for the individual lines, one can see from figure (6c), for example that a receiver operating at 0.88 MHz and located at 50 feet away from the center of line A.1, would experience an F_a value of 90 dB. If the receiver is moved from that location to a location 500 feet away from the line, it would experience an F_a value of 82 dB which is 8 dB less than that value obtained at the first location resulting in a greater S/N ratio and improved radio reception.

Chapter V

SUMMARY AND CONCLUSIONS

5.1 SUMMARY

Power lines are a source of interference to radio signals and digital communication systems. The radio interference generated from power lines is due to corona discharge and gap type noise or microsparks. Radio interference is only defined in statistical terms, as many investigators [2], [8], [10]-[16] and [19],[20] have shown. In order to perform a statistical analysis of RI, a large number of samples of this interference from a large number of lines, during different operating conditions, must be available.

To collect the data base required for the analysis, forteen test sites were selected on the Manitoba Hydro System in the rural area surrounding the City of Winnipeg. Sites were selected so that no other sources of interference such as car ignition noise, commercial radio stations and other power lines, were present at the test locations and frequencies. Approximately ten visits were made to each site over a one year period. Measurements of RI were performed over a frequency range 0.3 to 32 MHz using a Singer noise detector meter model NM-26T coupled through a matching network to a nine foot long monopole rod antenna (model 93049-1). The measurement equipment was transported and used in a van which had a mobile telephone, through which power line data (voltage, current and power) and weather conditions were collected.

The data base collected for the rms noise voltge and its voltage deviation were entered into computer files. Computer programs were written to calculate the effective antenna noise factor, F_a, which is the parameter universally used to compare noise produced from different sources. F_a was calculated at all nine test frequencies (0.343, 0.49, 0.88, 1.8, 3.4, 5.6, 10.03, 18.62 and 30.62 MHz) for each power line, at each of the five test locations. These locations were 50, 100, 150, 300 and 500 feet away from the center of the line, perpendicular to it.

Linear regression was applied to F_a to produce prediction models for each of the surveyed transmission lines. These models were obtained for F_a with respect to parameter such as frequency, distance and line voltage. The models can be used to predict the amount of radio signal degradation due to RI from power lines similar to those surveyed.

The voltage deviation, V_d, which identifies the type of noise received, was obtained by direct measurements. V_d variation with frequency at the five test locations for each site was obtained by applying the linear regression technique to the raw V_d values.

The relationship between F_a and line voltages was also determined using the linear regression technique. Effects of rain, wet snow and fair weather on the noise levels received from site B.3 (115 KV) were investigated.

5.2 CONCLUSIONS

This thesis presents an investigation of the characteristics of RI due to high voltage transmission lines in the high frequency bands extending up to 32 MHz. Mathematical models are obtained from the data base collected for F_a and V_d to predict the RI from different classes of power lines, classed according to line voltage.

Frequency, distance and voltage are the parameters that significantly affected the noise levels. Frequency is the parameter which has the greatest effect on the noise levels. The dramatic decrease in noise levels with the increase in frequency is seen from figures (5a-1) and figures (6a-1), whereas, the distance parameter displays a lesser effect on noise levels. From figures (7) and (8), it is seen that the noise levels increase with the increase in line voltage. The only exception of this, is the 66 KV line class that produced noise levels 6 dB greater than the 115 KV class . The unloaded line at site M.1 (66 KV) was found to be much noiser than the loaded site on the same line M.2 (66 KV). The difference was 23 dB higher. The relationship between noise levels and line loading was not obtained, but a measure of such a relationship should provide useful results in further specifying the noise associated with power lines. This relationship should be investigated in future studies. Another relationship that should be investigated is that of the voltage deviation with frequency. This relation should be researched using a higher order approximation technique (of order greater than linear regression).

Weather is another factor which affected the noise levels. It has been shown that during rain and wet snow, the noise levels received from site B.3 (115 KV) were higher than those values obtained during fair weather. This is mostly due to the increase in corona discharge, as water droplets enhance the electric field to produce corona at normal operating voltages.

The objectives of this study, mainly to perform measurements of RI from power lines and to obtain prediction models of the various classes of power lines, were achieved. The prediction models obtained for F_a versus frequency and distance are of most use in an environment similar to that surveyed.

APPENDIX A

LINEAR REGRESSION COEFFICIENTS

The least squares method is the method used to obtain the linear regression model coefficients. This method requires that the squared errors between data points and their estimated values have a minimum value. From figure (13), the error is given by:

$$r_i = (y_i - y)$$

$$\sum_{i=1}^{N} r_i^2 = \sum_{i=1}^{N} (y_i - y)^2$$

We have:

$$y = a + bx \ .$$

Thus,

$$R^2 = \sum_{i=1}^{N} r_i^2 = \sum_{i=1}^{N} (y_i - (a + bx_i))^2 \quad .$$

For minimum error:

$$\frac{\partial R^2}{\partial a} = 0 \qquad \text{and} \qquad \frac{\partial R^2}{\partial b} = 0 \quad .$$

First:

$$\frac{\partial R^2}{\partial a} = 2\sum_{i=1}^{N} (y_i - (a + bx_i))$$

$$\sum_{i=1}^{N} y_i = \sum_{i=1}^{N} (a + bx_i)$$

$$= \sum_{i=1}^{N} a + b\sum_{i=1}^{N} x_i$$

$$\sum_{i=1}^{N} y_i = Na + b \sum_{i=1}^{N} x_i \quad . \tag{1}$$

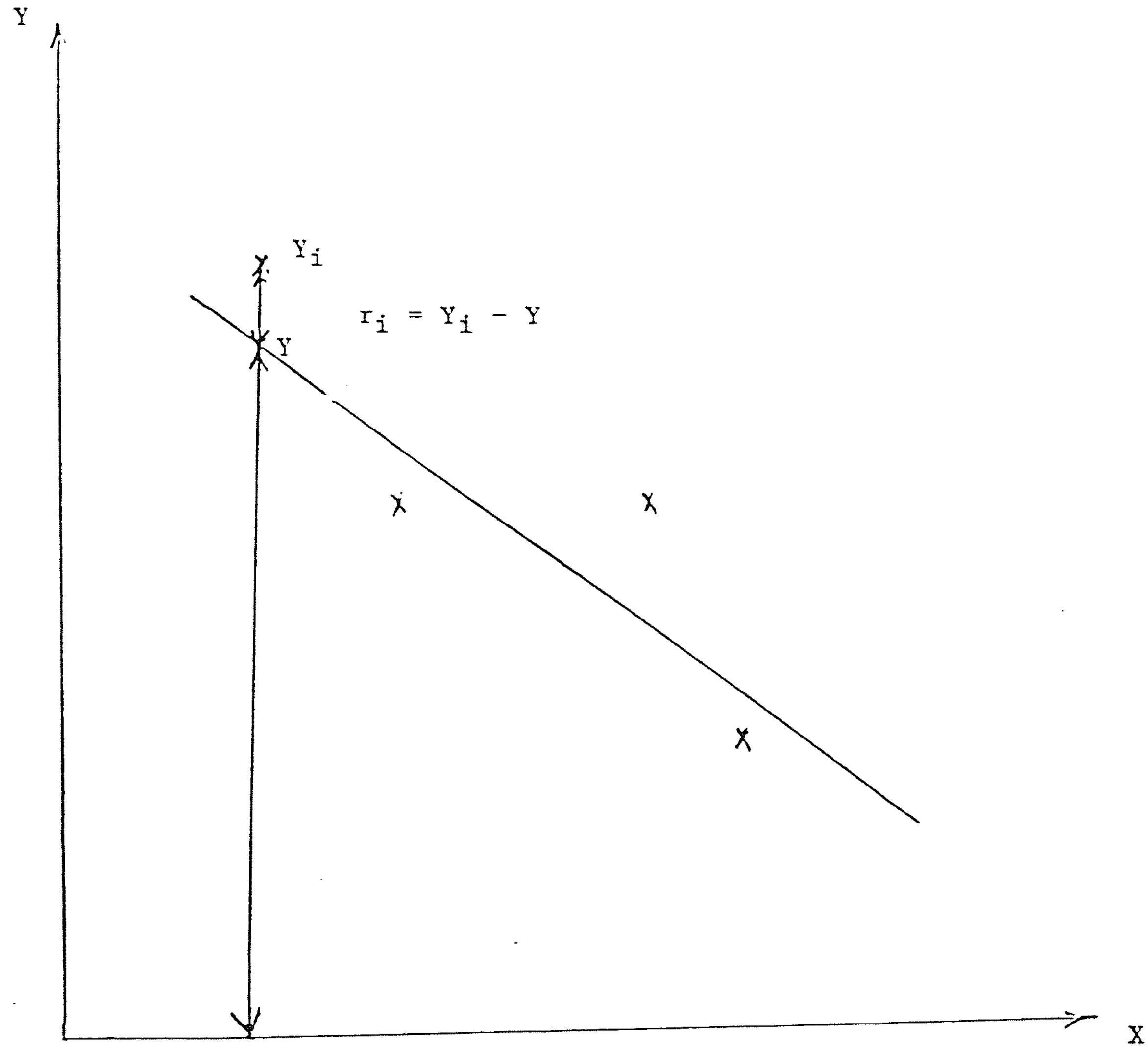

Figure (12)
Least squares method

Similarly:

$$\frac{\partial E^2}{\partial b} = 2 \sum_{i=1}^{N} ((y_i - (a + bx_i))\ x_i\ )$$

$$0 = \sum_{i=1}^{N} (y_i x_i - ax_i - bx_i^{\ 2})$$

$$\sum_{i=1}^{N} y_i x_i = a \sum_{i=1}^{N} x_i + b \sum_{i=1}^{N} x_i^2 \quad . \qquad (2)$$

Multiply equation (1) by Σx, equation (2) by N and subtract the first from the second to get:

$$b = \frac{N\Sigma XY - \Sigma X \Sigma Y}{N\Sigma X^2 - (\Sigma X)^2} \quad . \qquad (3)$$

Divide both the numerator and denomenator of equation (3) by N and putting $\bar{X} = \frac{\Sigma X}{N}$ and $\bar{Y} = \frac{\Sigma Y}{N}$ we write:

$$b = \frac{\Sigma XY - \frac{\Sigma X \Sigma Y}{N}}{\Sigma X^2 - \frac{(\Sigma X)^2}{N}} = \frac{\Sigma XY - N\bar{X}\bar{Y}}{\Sigma X^2 - N(\bar{X})^2} \quad . \qquad (4)$$

Substituting from (4) into (1), we get:

$$a = \bar{Y} - b\bar{x} \quad .$$

From equations (3) and (4), the slope of the linear regression model and the intersect with the Y axis are calculated respectively.

The calculation of the correlation coefficient from its definition can be obtained as follows:

By definition:

$$r = \frac{\Sigma (Y - \bar{Y}) (X - \bar{X})}{N \sigma_X \sigma_Y}$$

$$(X - \bar{X}) (Y - \bar{Y}) = XY - \bar{X}Y - \bar{Y}X + \bar{X}\bar{Y}$$

$$\Sigma (X - \bar{X}) (Y - \bar{Y}) = \Sigma (XY) - \bar{X} \Sigma Y - \bar{Y} \Sigma X + N\bar{X}\bar{Y}$$

$$\frac{\Sigma (X - \bar{X}) (Y - \bar{Y})}{N} = \frac{\Sigma (XY)}{N} - \bar{X} \frac{\Sigma Y}{N} - \bar{Y} \frac{\Sigma X}{N} + \bar{X}\bar{Y}$$

$$r = \frac{\Sigma XY}{N} - \bar{X}\bar{Y} - \bar{Y}\bar{X} + \bar{X}\bar{Y}$$

$$r = \Sigma \frac{XY}{N} - \bar{X}\bar{Y} .$$

Thus:

$$r = \frac{\Sigma \frac{XY}{N} - \bar{X}\bar{Y}}{\sigma_X \sigma_Y} .$$

REFERENCES

[1] Canadian Electrical Association, "A Report On The Stat-OF-The Art of the Environmental Effects of Transmission Lines, Research Contract # 78-79, March 31, 1979.

[2] IEEE Radio Noise Subcommittee Report, "Radio Noise Design Guide For High Voltage Transmission Lines", IEEE Trans. On Pas, Vol. 90, No. 2, March/April 1971, pp. 833-42.

[3] H. H. Newel, T. W. Liao and F. W. Warburton, "Corona And RI Caused By Particles On Or Near EHV Conductors", Part I- Fair Weather, IEEE Trans. PAS, Vol. 86, Nov.1967., pp. 134.

[4] L. Boulet et al., "Environmental Studies Of Radio Interference From Conductors And Hardware", CIGRE Paper 408, 1966.

[5] F. Hirsch, e. Schefer, "Progress Report On The HVDC Test Line Of The 400 KV Forschungsgemein Schaft Corona Losses And Radio Interference", IEEE Trans. On PAS, Vol. 88, No. 9, July 1969, pp. 1061-69.

[6] W. Janischewskyj, "Characteristics Of RI And TVI Sources", IEEE Tutorial Course: The Location, Correction Of RI And TVI Sources From Overhead Power Lines. Course Text 76 CH 1163-5-PWR, 1976.

[7] W. Janischewskyj, J. Beattie, "Effects Of Humidity Upon Discharge Processes Of Negative A.C Corona", IEEE Conference Publication, No. 90, 2nd International Conference On Gas Discharges, London, England, pp. 391-93.

[8] O. Nigol, "Analysis Of Radio Noise From High Voltage Lines." I- "Meter Response To Corona Pulses", IEEE Transactions, Power apparatus and systems, Vol. 83, May 1969.

[9] IEEE Radio Noise Subcomittee Report, "Radio Noise Design Guide For High Voltage Transmission Lines", IEEE Transactions, Power apparatus and systems, Vol. 90, March/April 1971.

[10] Wilfred R. Lauber and Jean M. Bertrand, "Preliminary Urban VHF/UHF Radio Noise Intensity Measurements In Ottawa, Canada", A paper presented at thed second symposium and technical exhibition on electromagnetic compatibility. 28-30 June 1977.

[11] Lauber, W. R., "Mill Cove High Frequency Radio Noise Survey", CRC Report No. 1263, Ottawa, November 1974.

[12] Lauber, W. R., L. R. Bode and J. M. Bertrand, "High Frequency Radio Noise Survey At Three Communication Sites In Ottawa Area", CRC Report No. 1294, Ottawa, August 1976.

[13] Lauber, W. R., "Amplitude Probability Distribution Measurements At The Apple Grove 775 KV Project", IEEE Transactions on power apparatus and systems, On Pas, Vol. 95, No.4, July/August 1976, pp. 1254-1266.

[14] Victor Herak and A. Kirk, "Power Line Noise In The City Of Winnipeg 285 KHz to 950 MHz", Project No. 88D-001, August 1977.

[15] W. R. Goddard, E. Bridges, W. M. Boerner, "Measurement And Study Of Radio Noise From Electric Power Lines In The Central Canada Region", Preliminary Report On Contract No OST78-00083, April 1979.

[16] E. Bridges, W. R. Goddard, T. Cad and W. M. Boerner, "Measurement And Study Of Radio Noise From Electric Power Lines In The Central Canada Region", To be Presented At IEEE International Symposium On Electromagnetic Compatability, October 1980.

[17] Henry L. Alder and Edward B. Roessler, "Introduction to Probability and Statistics", San Francisco and London: W. H. Freeman and Company, 1961.

[18] Ralph H. Pennington, "Introductory Computer Methods and Numerical Analysis", London: Collier Macmillan Limited, 1970.

[19] Alan Stuart, "Regression Estimation From Grouped Observations. Being Number Thirty Three Of Griffin's Statistical Monographs & Courses", London: Charles, Griffin & Company Limited, 1973.

[20] CCIR Documents Of The Xth Plenary Assembly, "World Distribution And Characteristics Of Atmospheric Radio Noise", Report 322, Geneva, 1964.

[21] W. E. Pakala, "Radio Noise Measurements On Overhead Power Lines From 2.4 To 800 KV." , IEEE Transaction On PAS, Vol. 90, PP. 1155, 1971.

[22] R. F. Harrington, "Time Harmonic Electromagnetic Fields" , PP 223, 1961.